Atmos. Chem. Phys. Discuss., 10, 18255–18313, 2010
www.atmos-chem-phys-discuss.net/10/18255/2010/
doi:10.5194/acpd-10-18255-2010

Atmospheric Chemistry and Physics Discussions

Direct satellite observation of lightning-produced NO_x

S. Beirle[1], **H. Huntrieser**[2], **and T. Wagner**[1]

[1]Max-Planck-Institut für Chemie, Mainz, Germany
[2]Institut für Physik der Atmosphäre, Deutsches Zentrum für Luft- und Raumfahrt (DLR), Oberpfaffenhofen, Germany

Received: 9 July 2010 – Accepted: 21 July 2010 – Published: 2 August 2010

Correspondence to: S. Beirle (steffen.beirle@mpic.de)

Published by Copernicus Publications on behalf of the European Geosciences Union.

Abstract

Lightning is an important source of NO_x in the free troposphere, especially in the tropics, with high impact on ozone production. However, estimates of lightning NO_x (LNO_x) production efficiency (LNO_x per flash) are still quite uncertain.

In this study we present a systematic analysis of NO_2 column densities from SCIAMACHY measurements over active thunderstorms, as detected by the World-Wide Lightning Location Network (WWLLN), where the WWLLN detection efficiency was estimated using the flash climatology of the satellite lightning sensors LIS/OTD. Only events with high lightning activity are considered, where corrected WWLLN flash rate densities inside the satellite pixel within the last hour are above $1/km^2/h$. For typical SCIAMACHY ground pixels of $30\times60\,km^2$, this threshold corresponds to 1800 flashes over the last hour, which, for literature estimates of lightning NO_x production, should result in clearly enhanced NO_2 column densities.

From 2004–2008, we find 287 coincidences of SCIAMACHY measurements and high WWLLN flash rate densities. For some of these events, a clear enhancement of column densities of NO_2 could be observed, indeed. But overall, the measured column densities are below the expected values by more than one order of magnitude, and in most of the cases, no enhanced NO_2 could be found at all.

Our results are in contradiction to the currently accepted range of LNO_x production per flash of 15 $(2–40)\times10^{25}$ molec/flash. This probably partly results from the specific conditions for the events under investigation, i.e. events of high lightning activity in the morning (local time) and mostly (for 162 out of 287 events) over ocean.

Within the detected coincidences, the highest NO_2 column densities were observed around the US Eastcoast. This might be partly due to interference with ground sources of NO_x being uplifted by the convective systems. However, it could also indicate that flashes in this region are particularly productive.

We conclude that current estimates of LNO_x production might be biased high for two reasons. First, we observe a high variability of NO_2 for coincident lightning events. This

ACPD
10, 18255–18313, 2010

high variability can easily cause a publication bias, since studies reporting on high NO_x production have likely been published, while studies finding no or low amounts of NO_x might have been rejected as errorneous or not significant. Second, many estimates of LNO_x production in literature have been performed over the US, which is probably not representative for global lightning.

1 Introduction

Nitrogen oxides (NO and NO_2, summarized as NO_x) play an important role in atmospheric chemistry by driving ozone formation and influencing the OH concentration. Lightning constitutes an important natural source of NO_x, hereafter denoted as Lightning NO_x (LNO_x). LNO_x is directly produceded in the upper troposphere where background levels of NO_x are generally low and the lifetime of NO_x is of the order of a few days, i.e. several times longer than for the boundary layer (hours). Hence its impact on ozone production and oxidizing capacity is quite high (e.g., Labrador et al., 2005), compared to its fraction of total NO_x production. However, estimates of the total annual NO_x release by lightning are still uncertain, and literature results differ significantly, though they seem to be converging on the range of 2–8 Tg N yr^{-1} (Schumann and Huntrieser, 2007, and references therein).

In recent years, satellite measurements of NO_2 came up, which have provided a valuable dataset of tropospheric NO_x with global coverage. Nadir-viewing UV-Vis satellites like GOME(1&2), SCIAMACHY, or OMI, allow the retrieval of total slant column densities (SCDs), i.e. integrated concentrations along the effective light path, of several atmospheric trace gases. For NO_2, the retrieval of tropospheric SCDs (TSCDs) requires the subtraction of the stratospheric column. Tropospheric *vertical* column densities (TVCDs), i.e. vertically integrated concentrations, are obtained by consideration of radiative transfer, involving information of ground albedo, aerosols and clouds, and the NO_2 vertical profile. Tropospheric NO_2 data from satellite has been successfully used for the investigation of NO_x sources and chemistry in many studies (see e.g. Wagner,

ACPD
10, 18255–18313, 2010

2008; Martin et al., 2008, and references therein).

Several studies have also investigated and quantified LNO_x using satellite NO_2 observations. Beirle et al. (2004) found a correlation of flash counts from the Lightning Imaging Sensor (LIS) with monthly mean NO_2 TSCDs from GOME over Australia, and estimated the mean LNO_x production as 2.8 (0.8–14) Tg N yr^{-1}. Boersma et al. (2005) reported on an increase of mean NO_2 TVCDs over high convective clouds, and estimated the mean LNO_x production as 1.1–6.4 Tg N yr^{-1} from correlations of NO_2 TVCDs with parameterized flash rates. Martin et al. (2007) constrain the mean annual LNO_x production to 6 (4–8) Tg N by comparing satellite observations of NO_2, O_3 and HNO_3 to a global chemical transport model. (Even the chemistry of the middle atmosphere is affected by lightning as has been shown by Arnone et al. (2008) who report on enhancements of NO_2 from MIPAS of about 10% around the stratopause due to sprites.)

These approaches consider mean NO_2 column densities for time periods of months to years. As lightning activity peaks in the late afternoon, whereas current UV/vis satellite instruments measure NO_2 in the morning (GOME, GOME2, SCIAMACHY) or shortly after noon (OMI), the potentially present LNO_x is – to large part – aged. Consequently, spatial patterns of the LNO_x produced by individual thunderstorms are lost, and the averaged NO_2 enhancements are smeared out, and generally low. Thus, the impact of systematic errors within the retrieval is quite high. Especially uncertainties of the estimation of stratospheric column densities of the order of 0.5×10^{15} molec/cm^2 (Boersma et al., 2004) can strongly bias spatial averages over clean regions. Also spectral interferences of ground absorption features with the NO_2 cross-section can lead to biased SCDs of the same order of magnitude (Beirle et al., 2010). Finally, to estimate the NO_x production from mean NO_2 VCDs, information on the NO_x *lifetime* is required (or a chemical model has to be involved), which is also uncertain and, as a further complication, strongly height dependent. These difficulties can be overcome by investigating *direct* observations of freshly produced LNO_x over active thunderstorm: Beirle et al. (2006) analyzed a mesoscale convective system in the Gulf of Mexico in August 2000, which coincides with the GOME overpass in space and time. Individual GOME

ACPD
10, 18255–18313, 2010

TSCDs are up to 10×10^{15} molec/cm^2. By roughly estimating the satellite's sensitivity for NO_2 in cumulonimbus clouds, and relating the observed NO_2 TSCDs to flashes detected by the US National Lightning Detection Network NLDN, a mean LNO_x production of 90 (32–240) mol/flash, corresponding to $5.4\,(1.9–14.5)\times10^{25}$ molec/flash, was derived. Note that for this estimate it was assumed that the enhanced NO_2 TSCD is completely due to lightning. In case of contributions of anthropogenic outflow from the US, the estimated LNO_x production would be even lower. Bucsela et al. (2010) analyzed OMI NO_2 TVCDs within the TC4 campaign around Costa Rica and report on four days with lightning-related enhancements of OMI NO_2 TVCDs. Involving in-situ NO_2 profile measurements from the DC-8 aircraft missions, and flash counts from lightning networks, they estimate LNO_x production per flash in the range of ≈100–250 mol/flash, which corresponds to $6–15\times10^{25}$ molec/flash.

For such direct observations, which generally imply satellite measurements under cloudy conditions, the aspect of the sensitivity (i.e. the air mass factor AMF) is particularly important for quantitative analyses. Hild et al. (2002) analyzed AMFs for NO_2 for cumulonimbus clouds, and found high sensitivity for NO_2 at the cloud top, decreasing (approximately linear) to almost zero at the cloud bottom. Beirle et al. (2009) calculated NO_2 AMFs for an ensemble of lightning scenarios from a cloud-resolving model, and in particular established a link between the measured NO_2 TSCD to the actual NO_x TVCD by considering the height-dependent NO_x partitioning. Since the NO_2/NO_x ratio decreases with altitude due to decreasing temperatures and increasing actinic flux, the sensitivity for NO_x, in contrast to the box-AMFs for NO_2, is not highest at the cloud top, but instead in the middle of the cloud. As result from Beirle et al. (2009), an overall quite high sensitivity of satellite observations for LNO_x was determined. This leads to the straightforward expectation that events of high lightning activity, which will be defined quantitatively in Sect. 2.4, should produce an amount of LNO_x that would result in enhanced NO_2 TSCDs clearly detectable from space.

In this study, we make use of the global dataset of SCIAMACHY NO_2 TSCDs, combined with global lightning data provided by WWLLN, to systematically search for

ACPD
10, 18255–18313, 2010

events of high lightning activity and check our current understanding of LNO_x production. In addition, the global perspective allows to investicate possible systematic differences in regional LNO_x productivity.

2 Data and methods

We perform a systematic analysis of NO_2 column densities during and shortly after events of high lightning activity. NO_2 data is derived from the SCIAMACHY instrument (Sect. 2.1), where the specific viewing conditions during thunderstorms and their impact on the sensitivity of satellite measurements is taken into account (Sect. 1). Lightning information is taken from the World-Wide Lightning Location Network (WWLLN, Sect. 2.3), which provides global and continuous lightning information. For quantitative interpretation of the WWLLN flash counts, the WWLLN detection efficiency (DE) is estimated using the flash climatology derived from OTD/LIS satellite measurements. In Sect. 2.4, the definition for "high" lightning activity is given. Finally, in Sect. 2.5, the observed NO_2 TSCDs are set in relation to the number of WWLLN flashes, and the LNO_x production efficiency is derived for each event.

To assist the reader, Table 1 gives an overview of the acronyms and symbols used in this study.

2.1 SCIAMACHY NO_2 column densities

The Scanning Imaging Absorption spectroMeter for Atmospheric CHartographY, SCIAMACHY (Bovensmann et al., 1999), was launched onboard the ESA satellite ENVISAT in March 2002. ENVISAT orbits the Earth in a sun-synchronous orbit with a local equator crossing time of about 10:00 a.m. in descending node.

SCIAMACHY measures Earthshine spectra from the UV to the NIR with a spectral resolution of 0.22–1.48 nm. In nadir geometry, the instrument performs an across-track scan of about ±32°, equivalent to a swath-width of 960 km. The footprint of a sin-

ACPD
10, 18255–18313, 2010

gle nadir observation is typically $30 \times 60\,km^2$. Global cover of nadir measurements is achieved after 6 d.

Total SCDs of NO_2 are derived from SCIAMACHY nadir spectra using Differential Optical Absorption Spectroscopy DOAS (Platt and Stutz, 2008). Cross-sections of O_3, NO_2 (at 220 K), O_4, H_2O and CHOCHO are fitted in the spectral range 430.8–459.5 nm. In addition, Ring spectra, accounting for inelastic scattering in the atmosphere (rotational Raman) as well as in liquid water (vibrational Raman), an absorption cross-section of liquid water, and a polynomial of degree 5 are included in the fit procedure. A daily solar measurement is used as Fraunhofer reference spectrum.

The stratospheric fraction of total SCDs as function of latitude is estimated in a reference sector over the remote Pacific. Longitudinal variations of the stratospheric field, which occur especially in cases of asymmetric polar vortices, are corrected using SCIAMACHY limb observations as described in Beirle et al. (2010). After substracting the estimated stratospheric field from total SCDs, tropospheric SCDs (TSCDs) of NO_2 are derived.

2.2 Sensitivity of satellite observations for freshly produced LNO_x

For a quantitative interpretation of NO_2 TSCDs for lightning conditions, the extreme viewing conditions under cumulonimbus clouds have to be considered. For this purpose, Beirle et al. (2009) determined the "sensitivity" E, defined as ratio of NO_2 TSCD (i.e. the NO_2 SCD observed from space after stratospheric correction) and the TVCD of NO_x (i.e. the vertically integrated NO_x column, which directly results from the totally released LNO_x):

$$E := S_{NO_2}/V_{NO_x}. \quad (1)$$

Values for E were calculated using profiles of NO_2, NO_x, and hydrometeors from a cloud-resolving chemistry model for a simulation of a one week thunderstorm episode in the TOGA COARE/CEPEX region, combined with a radiative transfer model.

ACPD
10, 18255–18313, 2010

Note that for the calculation of S_{NO_2}, and thus E, in Beirle et al. (2009), the height-dependencies of the NO_2 sensitivity (or box-AMF) and of the NO_2/NO_x partitioning are accounted for *simultaneously*. The NO_2/NO_x ratio at the ground is about 0.7 (cloud free) up to 1 (clouded). It decreases approximately linearly with altitude down to values below 0.1 in the upper troposphere due to the high actinic flux and the low temperatures. Box-AMFs for NO_2 are almost zero below a cloud, and reach values of more than 4 at the top of a cb cloud due to multiple scattering (compare Hild et al., 2002).

As a consequence of these opposite height dependencies of the NO_2/NO_x ratio and the NO_2 box-AMF, the sensitivity E of satellite observations for LNO_x is

- low (<0.1) at the cloud top and above: box-AMFs for NO_2 are high, indeed, but there is almost no NO_2 to be seen due to the low $[NO_2]/[NO_x]$ ratio <0.1.
- maximum (≈1) in the cloud middle: here, NO_2 box-AMFs are still high (≈2), and there is enough NO_x present in form of NO_2 to be detected from space.
- decreasing towards the cloud bottom, due to the decrease in NO_2 box-AMFs.
- almost zero below the cloud due to the cloud shielding.

For the simulated LNO_x profiles, Beirle et al. (2009) find a mean sensitivity E of 0.46 with a standard deviation of 0.09. I.e., for a true LNO_x TVCD of 1×10^{15} molec/cm^2, it is expected to observe a NO_2 TSCD of 0.46×10^{15} molec/cm^2 from satellite. Remarkedly, the values for E are almost independent on cloud optical thickness, i.e. they are valid for the core, the anvil, and the outflow of a thunderstorm likewise. This is a consequence of the effects of clouds on both, the $[NO_2]/[NO_x]$ ratio and the NO_2 box-AMF, combined with the different mean NO_x profiles for core (almost homogeneous) and outflow (C-shape), within the model study.

In the following, we apply this estimate of E=0.46 for the transformation of measured NO_2 TSCDs into NO_x TVCDs.

ACPD
10, 18255–18313, 2010

2.3 The WWLLN

For the identification of satellite measurements of NO_2 coinciding with (or shortly after) events of high lightning activity, *continuous* lightning data is required. This is provided by the ground-based WWLLN.

WWLLN started operation as global lightning location network in 2003 (Dowden et al., 2008). It consists of several sensors around the world detecting "sferics" caused by lightning in the very low frequency (VLF) band (6 to 22 kHz). A lightning stroke is identified if a sferic is detected by at least 5 WWLLN stations, and localized using the time of group arrival (Dowden et al., 2002).

The detection efficiency (DE) of WWLLN depends e.g. on the flash type (cloud-to-ground vs. intra-cloud): WWLLN is primarily focussing on the detection of cloud-to-ground (CG) flashes with well-defined return stroke peak currents (Rodger et al., 2006). However, Jacobson et al., 2006, showed that WWLLN is also capable of detecting intra-cloud (IC) flashes with similar DE, as long as their peak current is sufficiently high.

A further critical parameter for a stroke being detected by WWLLN is also its peak current: WWLLN only detects strokes with peak currents above ≈10 kA, with increasing DE for peak currents up to 50 kA. Above this level, the DE is not increasing further (Jacobson et al., 2006; Rodger et al., 2006, 2009).

In addition, the DE varies regionally and temporally, depending on the number and spatial distribution of participating ground stations. Note that the DE increased from 2007 on by about 63% (relative) due to an algorithm upgrade (Rodger et al., 2009).

In order to quantify the actual number of flashes, we estimate the WWLLN DE as function of time and place. For this purpose, calibrated global lightning information is needed, which is provided by the flash climatology from combined OTD/LIS measurements (OTD: Optical Transient Detector; LIS: Lightning Imaging Sensor). We thus relate annual mean WWLLN flash rate densities (FRD) $F^{\text{annual}}_{\text{WWLLN}}$, i.e. flashes per area and year, to the corresponding climatological LIS/OTD flash rate densities F_{LIS}. For each year, we define this ratio as "climatological" WWLLN DE D_{clim}, given as function

ACPD
10, 18255–18313, 2010

of place.

$$D_{\text{clim}} := F^{\text{annual}}_{\text{WWLLN}} / F_{\text{LIS}}. \quad (2)$$

Note that we thereby (a) assume that the OTD/LIS climatology is "true" and (b) implicitely also correct for the dependencies of WWLLN DE on flash type, since LIS and OTD are sensitive for CG and IC flashes likewise.

Regions with low LIS/OTD FRD (F_{LIS}<1/year/km^2) are skipped (i.e., D_{clim} is not defined) to avoid small denominators.

For the quantification of flashes within the satellite pixel (see Sects. 2.4 and 2.5), we define a corrected WWLLN FRD $F^{\text{corr}}_{\text{WWLLN}}$ as

$$F^{\text{corr}}_{\text{WWLLN}} := F_{\text{WWLLN}} / D_{\text{clim}}. \quad (3)$$

To limit the upscaling of very low FRD, we only consider regions with D_{clim}>1% in the following.

A detailed description of our procedure to estimate annual WWLLN DE, including maps of the resulting DEs and comparisons to literature estimates of DE, are presented in Appendix A.

2.4 Definition of "high" lightning activity

In this study, we focus on SCIAMACHY NO_2 measurements coinciding in time and space with high lightning activity, also simply denoted as "events" hereafter. The WWLLN flash counts within each satellite groundpixel are summed up over the last 60 min prior to the SCIAMACHY measurement. A coincidence is considered to be an "event" if the respective flash rate density $F^{\text{corr}}_{\text{WWLLN}}$, i.e. the sum of measured WWLLN flashes within the satellite pixel over the last 60 min, scaled by $1/D_{\text{clim}}$, is above 1/km^2/h. For a typical SCIAMACHY ground pixel of 30×60 km^2, this FRD corresponds to 1800 flashes within the last hour.

ACPD
10, 18255–18313, 2010

Note that only flashes of the previous 60 min are counted; older flashes are not considered. Thus, the derived FRD is rather a *lower bound* for the actual number of flashes.

Events close to anthropogenic sources of NO_x are skipped to avoid interference from ground NO_x sources being potentially uplifted by convective systems. This is implemented by defining a "pollution mask" from the mean global distribution of NO_2 TSCDs, which basically masks out polluted regions in continental US, Europe, and China. However, interference of anthropogenic NO_x may still occasionally occur in case of transport in the upper troposphere, and also NO_x from biomass burning or soil emissions might interfere with LNO_x.

By our rigid definition of high lightning activity, however, we particularly focus on *fresh* LNO_x, where we can expect a direct spatial correlation of flash occurence and the NO_2 signal.

2.5 Relation of NO_2 TSCD and WWLLN FRD

For the detected events, we relate the observed NO_2 TSCDs to the respective WWLLN FRD. We therefore assume that NO_x contributions from sources other than lightning are negligible, and that the loss of LNO_x due to chemical transformations or outflow/dilution can be neglected within the considered time period of 1 h and for the area of a SCIAMACHY ground pixel of $30 \times 60\ km^2$.

The NO_x TVCD V_{NO_x} due to lightning, i.e. the vertically integrated LNO_x concentration, is then given as

$$V_{NO_x} = F \times \Delta T \times P, \quad (4)$$

with F being the flash rate density (flashes per time per area), i.e. $F \times \Delta T$ being a flash density (flashes per area), and P the LNO_x production per flash, denoted as "Production Efficiency" (PE) below. In the review of Schumann and Huntrieser (2007), the best estimate for P is given as $15\,(2\text{–}40) \times 10^{25}$ molec $[NO_x]$/flash (Table 21 therein; note that this estimate is based on several studies with different methodology, and that for

ACPD
10, 18255–18313, 2010

the contributing field measurements, different lightning detecting systems have been used). For our threshold FRD of $1/km^2/h$ and the considered time period ΔT of 1 h, we thus expect a LNO_x TVCD of 15×10^{15} molec/cm^2. This corresponds to a NO_2 TSCD of 6.9×10^{15} molec/cm^2 (Eq. 1 with E=0.46). Such high NO_2 TSCDs are far above background levels (about $0–1\times10^{15}$ molec/cm^2) and would be clearly visible from space.

For each event, an individual PE P_{event} can be estimated from the measured NO_2 SCD and the derived WWLLN FRD, using Eqs. (4), (1) and (3):

$$P_{event} = \frac{V_{NO_x}}{F_{event} \times \Delta T} = \frac{S_{NO_2}/E}{F^{corr}_{WWLLN} \times \Delta T}. \quad (5)$$

Note that, by this definition, P_{event} is *overestimated* whenever lightning activity more than 1 h ago can not be neglected.

3 Results

A systematic search of NO_2 column measurements from SCIAMACHY for coincident lightning results in 287 events (as defined in Sect. 2.4) for the period 2004–2008. As expected, during (or shortly after) active thunderstorms, all satellite pixels for the detected events are cloud covered, with a mean FRESCO cloud fraction of 0.97 and a mean cloud height of 10.6 km (note that FRESCO cloud heights approximately correspond to the cloud *middle* (Wang et al., 2008), and all events are thus deep convective cases reaching the upper troposphere). Figure 1 shows the global distribution of the detected events. In addition, the derived Production Efficiency P_{event} (Eq. 5) is color-coded. Some selected events, which are discussed in detail below, are labelled by their event-ID (see also Table 2).

The spatial distribution of detected events is affected by D_{clim}, the pollution mask, and morning-time flash characteristics. Most events are found around the Carribean

ACPD
10, 18255–18313, 2010

Sea and in Indonesia/Australia, where WWLLDN DE is quite high (about 5% up to 20%), whereas only few events have been found in Central Africa, as a consequence of the DE threshold of 1%. The pollution mask removes some events in the continental South-Eastern US, Southern Europe, and South-East Asia. As the diurnal cycle of continental lightning activity has a distinct minimum around 10:00 a.m. LT, while it is rather flat over oceans, many events (162) have been found over ocean.

Events with relative high PE (red dots in Fig. 1) agglomerate east from Florida and in the northern Gulf of Mexico, where already a clear coincidence of lightning and strongly enhanced NO_2 TSCDs has been reported (Beirle et al., 2006). In contrast, in the northwest of Australia, where many events occured, values for P_{event} are rather low (blue).

Figure 2 shows a scatterplot of NO_2 TSCDs versus FRD for the detected events. The black line indicates the linear relation of Eq. 4 with a mean PE of $P = 15 \times 10^{25}$ molec/flash and a sensitivity E of 0.46. From Fig. 2, we can conclude the following basic results of our systematic search for LNO_x for events of high lightning activity:

1. The observed NO_2 TSCDs are generally far below the expected range of about $5–10 \times 10^{15}$ molec/cm^2 for a FRD of about 1, and the derived PE is far lower than values given in literature for most events.

2. In contrast to our expectations, NO_2 TSCDs are not correlated to WWLLN flash rate densities ($R = 0.04$). Therefore, we abandon to give an estimate of a "mean" PE in this study, which would be proportional to the slope of a linear fit to the data points in Fig. 2.

3. In *some* cases, a clear (spatial) coincidence of enhanced NO_2 due to lightning could be found, similar to the case study of enhanced NO_2 TSCDs observed from GOME in the Gulf of Mexico in August 2000 reported in Beirle et al., 2006. But for many events of high lightning activity, *no* enhanced NO_2 could be observed at all. We find 136 events with $P_{event} < 1 \times 10^{25}$ molec/flash.

ACPD
10, 18255–18313, 2010

Below we discuss some representative events, covering the range of observed PEs, in detail, and show spatial patterns of WWLLN flashes and NO_2 TSCDs. We focus on events with high WWLLN detection efficiencies, to limit upscaling of WWLLN FRD and the respective uncertainties. Consequently, most examples are taken after 2007, when WWLLN DE increased due to an improved algorithm (Rodger et al., 2009). Nevertheless, the general findings do not depend on D_{clim}, and events for lower DE are similarly variable.

We show illustrative examples for 3 general categories: (A) events with high NO_2 TSCDs and relatively high PE, (B) events with medium PE, and (C) events with PE of almost 0. For all examples, spatial patterns are displayed, showing the NO_2 TSCD, the respective cloud fraction (FRESCO, Wang et al., 2008), and the detected WWLLN lightning strokes, where colour indicates the flash time with respect to the SCIAMACHY overpass. Table 2 lists the properties for the selected events.

Category (A) High NO_2 TSCDs

Figure 3 (Event #115, south of Italy) and Fig. 4 (Event #191, east of Florida) show two examples of relatively high NO_2 TSCDs of 4.6×10^{15} molec/cm^2 and 5.8×10^{15} molec/cm^2 for the "events", i.e. the respective ground pixels with FRD >1/km^2/h. Production Efficiencies P_{event} are 3.5×10^{25} (#115) and 12.3×10^{25} (#191) molec/flash, respectively, almost reaching the best estimate given in Schumann and Huntrieser (2007).

However, in both cases, several neighbouring pixels show TSCDs of more than 6×10^{15} molec/cm^2 as well, whereas the lightning activity detected by WWLLN is rather concentrated at the event. The large plumes of enhanced NO_2 thus indicate contributions from other NO_x sources. In Appendix C, we analyse these events in more detail and discuss how far these enhanced NO_2 TSCDs can be explained by aged LNO_x or continental outflow of anthropogenic NO_x.

ACPD
10, 18255–18313, 2010

Category (B) Medium PE

Figure 5 (Event #261, Malaysia) and Fig. 6 (Event #225, Timor) show two illustrative examples for events with different lightning characteristics, where a NO_2 response to lightning could be identified. Event #261 is a mesoscale convective system with more than 500 km extent. The respective NO_2 TSCDs are slightly enhanced, and the maximum TSCD of 2.3×10^{15} molec/cm^2 coincides with the maximum FRD of 1.7/km^2/h. Spatial patterns of flashes and NO_2 TSCDs correlate well, supporting the interpretation of the NO_2 TSCDs to be due to lightning. However, the overall NO_2 TSCD is rather small compared to our expectation, and P_{event} is only 2.9×10^{25} molec/flash. Event #225 is an example for a very localized lightning event, where two neighbouring pixels exceed the FRD threshold of 1/km^2/h, but no lightning occurs outside. Again, NO_2 is enhanced at the event (and only there), but TSCDs are only moderately enhanced (2.4×10^{15} molec/cm^2 maximum), and P_{event} is 2.3×10^{25} molec/flash.

Category (C) "Zero" PE

In contrast to these examples, where we can at least claim a spatial correlation of flashes and enhanced NO_2, though the enhancement is lower than expected, Figs. 7 and 8 show events with no detectable NO_2 enhancement. Figure 7 (event #266, north of Venezuela) shows a NO_2 TSCDs of as few as 0.3×10^{15} molec/cm^2 for a FRD of 1/km^2/h; the neighbouring pixels show no indication of LNO_x outflow neither. Similarly, Fig. 8 displays event #208 (Malaysia) with a very high FRD of 5.8. NO_2 TSCDs are below 0.5×10^{15} molec/cm^2 for the respective ground pixel, whereas expected TSCDs according to Eqs. (4) and (1) would be as high as 40×10^{15} molec/cm^2, which is two orders of magnitude higher. P_{event} are 0.7×10^{25} and 0.2×10^{25} molec/flash, respectively, for both events.

ACPD
10, 18255–18313, 2010

4 Discussion

We performed a systematic search for satellite NO_2 observations coinciding with high lightning activity. In essence, the observed NO_2 TSCDs are generally far lower than expected, and show no correlation with WWLLN flash counts. Our findings are even more surprising given the fact that we do not consider flashes "older" than one hour and should thus estimate an *upper* bound of LNO_x production, since our estimate of flash counts is a lower bound.

In the following, we discuss the different event categories for the examples shown in Sect. 3. We investigate how far our results might be affected by the assumptions and characteristics of

- the NO_2 retrieval (Sect. 4.1),
- the satellites' sensitivity for lightning NO_x (Sect. 4.2),
- the WWLLN DE (Sect. 4.3),
- our definition of high lightning activity (Sect. 4.4),
- or our calculation of the PE (Sect. 4.5).

Finally, we discuss possible impacts of the observed high variability of PE on estimates of LNO_x production in literature (Sect. 4.6), and evaluate possible reasons which might cause these differences in PE (Sect. 4.7).

Category (A) High NO_2 TSCDs

As shown in Fig. 1, most events of (relatively) high P_{event} are observed in the Gulf of Mexico and east from Florida. This possibly indicates that PE is above average for the US, where deep convective updraft speeds are particularly high (Del Genio et al., 2007) and extreme precipitation is relatively frequent (Zipser et al., 2006). In fact, many

ACPD
10, 18255–18313, 2010

reports of high PE in literature are based on measurements over the US, e.g. Hudman et al. (2007) ($P \approx 30 \times 10^{25}$ molec/flash) or Langford et al. (2004) ($P \approx 58 \times 10^{25}$ molec/CG flash). Thus, one has to keep in mind that PE is regional dependent, and US estimates might not be representative globally.

For many of these high-PE events, like in event #191 (see Fig. 4), the patterns of enhanced NO_2 TSCDs cannot be explained by the flashes of the last hour. Thus, aged LNO_x, or the outflow of anthropogenic NO_x, lifted up by convection, probably contributes significantly to the observed NO_2 TSCDs. The latter has to be taken into account when quantifying LNO_x in the vicinity of "polluted" regions like the US east-coast, and might also partly explain the cluster of generally high PE found in this region. Indeed, we find indications for interference of anthropogenic NO_x and possibly also biomass burning NO_x for event #191, as shown in Appendix C. For such events where additional contributions from aged LNO_x or continental outflow of anthropogenic/biomass burning NO_x are not negligible (but hard to quantify), the estimated P_{event} are too high.

By our definition of events of high lightning activity and the calculation of P_{event}, we demand a spatial coincidence of lightning and NO_2 signal. It has to be noted that if we would instead consider the averaged NO_2 TSCD and the averaged FRD over a larger region of e.g. $300 \times 600\,km^2$ (i.e. 10×10 SCIAMACHY pixels), we would end up with a tremendously high PE of about 300×10^{25} molec/flash, despite the fact that large parts of the enhanced NO_2 plume show no spatial correlation with the observed flashes. The actual number of the estimated PE also strongly depends on the choice of the considered region. This underlines the importance of searching for consistent spatial patterns of NO_2 and FRD, and the need to analyze their relationship for individual satellite ground pixels instead of calculating large-scale spatial means.

Category (B) Medium P_{event}

In some cases, moderately enhanced NO_2 TSCDs have been found which show consistent spatial patterns with WWLLN flashes (see Figs. 5 and 6). These examples

ACPD
10, 18255–18313, 2010

demonstrate that, in some cases, it is possible to detect LNO_x from space. The values for P_{event} of about 2–3×10^{25} molec/flash are lower than the best estimate given in Schumann and Huntrieser (2007), but are within the range of uncertainty of 2–40×10^{25} molec/flash. Note that a value of P=3×10^{25} molec/flash would correspond to a total annual flash production of about 1 Tg N yr^{-1}.

Category (C) "Zero" P_{event}

The majority of events show no significantly enhanced NO_2 TSCDs at all, also causing a correlation coefficient of about 0 between FRD and NO_2 TSCD. The estimated values for P_{event} are orders of magnitude below the range reported in literature. From the quantities listed in Table 2, e.g. CTH, or the spatial patterns of flashes, we could not find an indication for what makes these "zero"-events different from the other.

In the following, we discuss how far our assumptions and the characteristics of the used datasets could explain our findings, focussing particularly on those "zero" NO_2 events.

4.1 NO_2 column densities

In this study we focus on NO_2 observations over active lightning systems, i.e. over cumulonimbus clouds. Such bright clouds may potentially affect the DOAS retrieval in two ways:

(a) Bright clouds might lead to saturation of the detected radiances, with hardly predictible consequences for the spectral retrieval of NO_2 SCDs. We thus checked the uncalibrated detector counts (binary units) per co-adding over high clouds, and found values lower than maximum counts measured at higher latitudes (with longer integration times). In addition, the fit residuals show no increased values over high clouds.

(b) Clouds affect the observed spectral structures in different ways, for instance by polarization effects (as SCIAMACHY is polarization dependent). Also inelastic scattering due to rotational and vibrational Raman is affected by clouds. Another effect

ACPD
10, 18255–18313, 2010

of clouds is the shielding of (spectral dependent) absorbers below, including spectral refelctance at the ground. In particular over oligotrophic oceans with low chlorophyll concentrations, absorption and vibrational Raman scattering in liquid water affects the NO_2 retrieval (see also Beirle et al., 2010). Changes of the DOAS-fit settings indeed reveal slight cloud interferences: The contrast of NO_2 SCDs for clouded versus cloud-free conditions over the remote Pacific depends on fit settings like polynomial degree and spectral window. However, these effects are only in the range of some 10^{14} molec/cm^2.

The derived TSCDs are – by definition of the stratospheric correction – *excess* TSCDs with respect to the Pacific. Consequently,

(a) negative (unphysical) TSCD occasionally occur in case of a local overestimation of the stratospheric column, and

(b) we generally underestimate real *clear-sky* NO_2 TSCDs by about 0.5×10^{15} molec/cm^2 (Martin et al., 2002). However, we can not simply add such an offset to the NO_2 TSCDs used in this study, since the NO_2 TSCDs of interest are observed under *cloudy* conditions with *modified* profiles due to convection, i.e. different sensitivity. However, this Pacific tropospheric background is quite small and does not affect our general findings.

4.2 Sensitivity of satellite observations for freshly produced LNO_x

For the translation of NO_2 TSCDs to NO_x TVCDs, we apply the sensitivity E of 0.46, as derived by Beirle et al., 2009 from a one-week episode of a thunderstorm simulation by a cloud resolving chemistry model. The model run covers all stages of thunderstorm evolution and thus allows to estimate E for a large variety of atmospheric conditions, while the simulated sensitivities for individual model columns show a surprisingly low variability. In particular, E is almost independent on cloud optical thickness, i.e. the sensitivities for core, anvil, and outflow regimes are quite similar. Above all, almost no pixels with zero sensitivity have been found, i.e. the model does not reproduce situations in which the LNO_x is completely hidden from the satellite's view. The derived sensitivities are also robust with respect to vertical shifts of the NO_x profile (see Beirle

ACPD
10, 18255–18313, 2010

et al., 2009).

Model results generally are subject to uncertainties, and the simulated (maritime) thunderstorm might not be representative for all thunderstorms investigated in this current study. However, the general pattern of the profiles of NO_2 box-AMFs (high at the cloud top and decreasing towards the cloud bottom) and of the NO_2/NO_x ratio (low at the cloud top and increasing towards the cloud bottom) is out of doubt, which automatically results in a maximum sensitivity at the cloud middle. As soon as LNO_x is present there, it becomes visible from space. Thus, the only plausible explanation for a scenario of completely "hidden" LNO_x would be a situation with all LNO_x placed below the cloud. Such LNO_x profiles might result from CG flashes occuring downwind (instead of inside) the updraft cores (compare Dye et al., 2000). However, such below-cloud LNO_x profiles are contrary to the commonly accepted "C-shape". In contrast, for LNO_x profiles with a large fraction of NO_x in the middle troposphere, as have been simulated by Ott et al., 2010, the sensitivity of satellite measurements for LNO_x would be even higher than 0.46.

4.3 WWLLN

The annual DE of WWLLN was estimated by a quite simple comparison of annual FRD to the LIS/OTD climatology. As the addition of stations to WWLLN can happen on any day within the year, the estimated annual mean DE maps are systematically too high for some regions up to the date when a new station is added, and too low afterwards. In addition, lightning statistics may not be sufficient after just one year, especially over oceanic regions. Both effects are definitely causing rather high error bars in the estimated DE, and thus would dampen the expected correlation of FRD to NO_2 TSCDs. However, these errors are to a large part of statistical nature, and thus can not explain the discrepancy of the absolute level of NO_2 TSCDs to our expectation. In addition, a particular focus on events for high DE of about 10% and more (in 2007 and 2008), where estimated FRD are more reliable, results in basically the same findings.

ACPD
10, 18255–18313, 2010

Due to the overpass time of SCIAMACHY at 10:00 a.m. LT, the selected events are morning-time thunderstorms, which may have specific characteristics. Thus, the derived climatological DE may be not representative for morning-time flashes. To further check the estimated DE of WWLLN D_{clim}, we also directly compared the number of individual flash counts from WWLLN to LIS flash counts whenever a coincident TRMM overpass occured. We therefore define "coincidence" as a LIS measurement containing the SCIAMACHY pixel center within a time window of 2 h before up to 1 h after the SCIAMACHY time. As LIS is an orbiting satellite, the observation duration at a specific location is rather short (about 1 min). Nevertheless, we found 42 out of 287 events, where coincident LIS measurements are available. For these coincidences, we compared LIS flash counts to WWLLN flash counts in the same time interval within the LIS field of view, thereby estimating also an *instantaneous* DE D_{inst}. The resulting values D_{inst} are presented and discussed in Appendix A.

Obviously, the DE D_{inst} derived from coincident LIS measurements is systematically higher (by a factor of about 3) than D_{clim} derived from the LIS/OTD climatology. This is an interesting finding, possibly indicating systematic differences of the morning-time flashes (about 10:00 LT) to average flash properties, e.g. in peak current or the CG/IC ratio.

One could argue that we thus have to modify our derived FRD F^{corr}_{WWLLN} by a factor of 3. However, the high values for D_{inst} compared to D_{clim} probably indicate enhanced peak currents of the respective flashes, which would directly affect the WWLLN DE (almost linearly for peak currents below 50 kA, Rodger et al., 2009). But in that case we would also expect that the respective flashes have LNO_x production P above average, since high current flashes also produce more LNO_x, which is also an almost linear effect, as shown in Wang et al. (1998). Thus, our expectation for the resulting NO_x TVCD (and thus the NO_2 TSCD) would remain more or less the same, as both effects (the increase in DE, thus the decrease in FRD, and the increase in PE) cancel each other out largely.

ACPD
10, 18255–18313, 2010

4.4 Definition of events of "high" lightning activity

One has to keep in mind that SCIAMACHY measurements are performed at about 10:00 a.m. LT. Thus, the selection of events of high lightning activity coinciding with SCIAMACHY is rather special, and the respective flashes may not be representative. In particular, most events have been found over ocean, where lightning activity is quite independent from daytime, while continental flashes show a strong afternoon peak (in addition, some continental events are skipped due to probable interference of anthropogenic NO_x).

Our indications for rather low LNO_x production may thus be specific for maritime morning-time flashes. However, we performed a similar case study using OMI observations (2:00 p.m.) which generally yields the same results (though the spatial correlation of TSCDs to FRD is more complex due to the smaller OMI ground pixel sizes).

4.5 Relation of NO_2 TSCDs and WWLLN FRD

For our estimation of the LNO_x production per flash, we assume that the produced LNO_x stays within the SCIAMACHY pixel for the considered time window of one hour. We thus neglect (a) chemical loss, which is well justified as the lifetime of NO_2 is of the order of days in the upper troposphere, and (b) dilution and outflow. We argue that this neglection is admissible, as the dimension of SCIAMACHY ground pixels is about $30 \times 60\,km^2$. The movement of the flash cluster, which can be tracked by the color-coded time in Figs. 4–8, may in fact "leave" the considered SCIAMACHY pixel occasionally (e.g. Fig. 6). However, this effect can not explain the findings of virtual no NO_2, like e.g. for event #266, as the NO_2 TSCDs for the respective neighbouring pixels are not enhanced neither. Even if we assume a "loss" of LNO_x of 50% due to transport, the discrepancy of our PE estimates to literature values remains.

ACPD
10, 18255–18313, 2010

4.6 High variability of PE

We observe a very high variability of NO_2 TSCDs and PE for the detected lightning events. This is, to some extent, in accordance to a very wide range of reported NO_x levels in and around thunderstorms and estimates of PE in literature (Schumann and Huntrieser, 2007). This wide range might be partly related to difficulties in aircraft observations, different lightning detection systems, and fundamental shortcomings in measurement techniques, and thus may just reflect the high observational uncertainties. But we might have to accept that lightning itself is a highly variable phenomenon, and PE is a highly variable quantity, varying strongly from thunderstorm to thunderstorm, and even from flash to flash. Consequently, one has to be aware that published estimates of PE are potentially biased towards too high values, since any finding of significantly enhanced NO_x in the vicinity of lightning is likely to be published, while measurements of no or low levels of NO_x might be discarded. This phenomenon is known as "publication bias" (e.g., Scargle et al., 2000).

Our category (B) results are in accordance to a LNO_x production of the order of $2–3\times10^{25}$ molec/flash, which is at the lower end of current estimates (Schumann and Huntrieser, 2007). However, the low PE values for category (C) results are far below any value reported in literature.

4.7 Factors determining PE

Several quantities have been discussed in literature to be determinative for the PE, i.e. the LNO_x produced per flash.

As a consequence of the Zel'dovich mechanism, PE increases with energy and peak current (Wang et al., 1998). Flashes of low peak current are thus less productive concerning LNO_x. This might in principle be a possible explanation for lightning without NO_2 production (category (C)). However, as we use FRDs based on WWLLN flash counts, we implicity (at least partly) account for this: a thunderstorm with flashes of low peak current would probably produce only a small amount of NO_x, but due to

ACPD
10, 18255–18313, 2010

dependency of WWLLN DE on peak current, only few flashes would be detected. The threshold of $F > 1/km^2/h$ thus selects, at the same time, events with many flashes as well as events with not too low peak currents. Since both, WWLLN DE and PE, increase almost linearly with peak current, we probably can not explain the category (C) events by less productive flashes due to low peak currents.

Huntrieser et al. (2008) report on relatively low PE for tropical thunderstorms during the TROCCINOX campaign in Brazil, in contrast to subtropical thunderstorms, and could relate this to a difference in average stroke lengths. They propose that tropical thunderstorms have generally shorter flash lengths, and are thus generally less productive with respect to LNO_x/flash, than subtropical thunderstorms, as a consequence of enhanced vertical wind shear of the latter. In Huntrieser et al. (2009) correlations of P with vertical wind shear are reported using in-situ measurements from the TROCCINOX and SCOUT-O_3 campaigns.

Indeed, Fig. 1 reveals a latitudinal dependency of P_{event}, showing higher values in the subtropics. However, this is mainly a consequence of the high values for P_{event} close to the US Eastcoast and in the Mediterranean, as represented by the category (A) examples #115 and #191. As discussed before, for these events, high NO_2 TSCDs are observed also for pixels without recent lightning activity, indicating the impact of aged LNO_x and/or outflow of anthropogenic pollution, so that the observed latitudinal dependency of P_{event} should not be overinterpreted. But at least most events with low P are indeed tropical events, which might thus be less productive due to low wind shears.

Huntrieser et al., 2009, also proposed that warm rain processes, which might be dominant for the tropical morning-time thunderstorms of this study, may result in very short flash components. I.e., though the detected events show, by definition, high FRD, these flashes might generally be less productive in producing NO_x compared to flashes for mixed-phase precipitation processes with probably longer flash channels. To check whether the detected events show mixed-phases, we investigated Polarization-Corrected Temperatures (PCTs) from the 37 and 85 GHz Radar TMI onboard TRMM, whenever coinciding (see Appendix B). For several events, quite low

ACPD
10, 18255–18313, 2010

PCTs are observed (<200 K down to 180 K at 37 GHz, and <100 K down to 70 K at 85 GHz), which classify the respective events as intense thunderstorms (Zipser et al., 2006) and indicate the presence of hail (Cecil, 2009). The PCT at 37 GHz is anticorrelated to Pevent (compare Fig. 17), i.e. PE tends to be higher for low PCT, which might indeed indicate a link of mixed-phase precipitation and lightning PE. This anticorrelation has to be investigated further in future.

Obviously, lightning is a very complex phenomenon, resulting in high variability of PE, and systematic dependencies on several parameters which are still poorly understood. Aiming for one single value of P (or, as a first specification, two universal values P_{IC} and P_{CG}) is probably not appropriate for the reproduction of global LNO_x production. The simple relation of P to flash properties like energy, peak current, or flash length is a first step, but increases the observational needs.

Further diversification of flash characteristics is probably needed. Rahman et al. (2007) measured the LNO_x production from rocket-triggered lightning and conclude that steady currents, and not return strokes, are the primary LNO_x producers. Cooray et al. (2009) analyzed the produced number of NO_x molecules for various flash processes in the laboratory, and confirm that return strokes produce relatively few NO_x, while other processes such as leaders or continuing currents are rather important.

Thus, one hypothesis which could explain the absence of LNO_x for events of high lightning activity might be the occurence of flashes with strong return strokes, making the flashes "visible" for LIS and WWLLN, but low steady currents (producing small amounts of LNO_x). However, this is quite speculative and hard to substantiate with currently available lightning datasets on global scale.

5 Conclusions

A systematic search for satellite measurements of NO_2 originating from "fresh" lightning (<1 h) results in 287 "events" of coincident SCIAMACHY measurements for high flash rate densities as observed by WWLLN. For each event, an individual estimate for the

ACPD
10, 18255–18313, 2010

Production Efficiency (PE, i.e. LNO_x production per flash) is derived.

Generally, the resulting values for PE are highly variable, and below literature values. Surprisingly, NO_2 column densities do not correlate with flash rate densities.

For some events, strongly enhanced NO_2 column densities are observed. However, the spatial pattern of NO_2 cannot be explained by the fresh flashes alone, but probably by aged LNO_x and/or continental outflow of anthropogenic pollution.

Several events show a good spatial correlation of flashes and enhanced NO_2 column densities; however, PE was rather low ($2–3\times10^{25}$ molec/cm^2), which would correspond – by simple extrapolation – to a global annual LNO_x production of the order of 1 Tg N.

The majority of the events has very low PE ($<1\times10^{25}$ molec/flash). We do not see any reason to abandon these events as artefacts or outliers. However, we could not find any characteristics of these less productive events which makes them different from the others, and find no plausible explanation for these events. Further investigations have to reveal how far these low estimates of PE are related to the selection of morning-time thunderstorms, mostly over oceans. From the continental events of this study, however, we come to essentially the same conclusions.

Overall, our results are not consistent with the current estimates of P of about 15 ($2–40)\times10^{25}$ molec/flash. While this might be related to the specifics of morning time flashes, it could also indicate that PE is overestimated in literature. We see two possible reasons for this:

1. As a consequence of the high variability of PE, published estimates might be biased high, as soon as they have been selective for thunderstorms with high PE, while studies resulting in low PE might have been discarded as non-significant or non-conclusive.

2. A large fraction of estimates of NO_x production by lightning is based on experiments performed in the US, for several reasons: there is a large scientific community, a good infrastructure (lightning networks, aircraft campaigns), and lightning activity is high. However, our study shows that PE around the US is highest glob-

ACPD
10, 18255–18313, 2010

ally. This might be related to higher flash lengths of subtropical thunderstorms, but also uplifted anthropogenic pollution might interfere. Consequently, extrapolations of PE estimates over the US to global scale are biased too high.

Obviously, the matter of NO_x production by lightning still leaves many questions open, and lightning characteristics are probably too complex to be reasonable represented by just one universal number for PE. Within the ongoing studies on LNO_x production, satellite measurements of NO_2 allow an independent approach, complementing laboratory and in-situ measurements.

Appendix A

Estimating the detection efficiency of WWLLN

A1 DE from LIS/OTD climatology

For a quantitative relation of NO_2 TSCDs to FRD, the number of flashes actually measured by WWLLN has to be scaled according to the respective detection efficiency (DE). Thus, estimates of WWLLN DE are required as function of time and place. For this purpose, we calculate mean annual FRD from individual WWLLN flash counts on a map of 1° resolution for each year 2004–2008, and set them in relation to the FRD from LIS/OTD climatology (LIS/OTD documentation, 2007) to define the climatological DE D_{clim} (see Eq. 2).

To avoid biased DE caused by strong localiced thunderstorms (which may potentially lead to high local FRD above average and thus to a too low DE estimate), both, LIS/OTD and WWLLN FRD are smoothed by a Gaussian function with σ=1.5°. We skip regions with $F_{LIS} < 1$ flashes/year/km^2, to avoid division by small numbers with respective high uncertainties.

Figures 12 and 13 show the resulting DE for 2005 and 2008 exemplarily. DE is highest over Australia and Indonesia, as WWLLN evolved from a regional network initiated

ACPD
10, 18255–18313, 2010

in New Zealand (Dowden et al., 2008). Over the years, the number of participitating stations increased from 19 (2004) to 30 (2007) (Rodger et al., 2009), which improves the DE also for other parts of the world, in particular for central and northern America.

The DE of 2005 can be compared to the estimate given in Rodger et al. (2006) (Figs. 13 and 14 therein), for April 2005, showing generally similar spatial patterns. However, a quantitative comparison also shows large deviations. Differences are expected for mainly two reasons: First, Rodger et al. (2006) estimate DE for one day (16 April 2005), while Fig. 12 shows our mean annual DE for 2005. Second, Rodger et al. (2006) explicitely estimate DE for CG flashes, while our climatological approach based on LIS/OTD is an "effective" DE for total (IC+CG) flashes. Consequently, we expect our DE to be lower by a factor of about 4 (for a IC/CG ratio of 3). One striking difference is that our estimated DE shows a clear land-ocean contrast, which is not visible in the estimate by Rodger et al. (2006). This is probably related to a land-ocean contrast in the DE of WWLLN, which is expected, since VLF radio waves propagate with less attenuation over seawater than over land. However, Lay et al. (2007) found only a small effect with DE over ocean being 13% higher (relative) than over land. The observed land-sea contrast might also be related to LIS/OTD characteristics, or a change in the IC/CG ratio.

Jacobson et al. (2005) investigate WWLLN DE for both IC and CG flashes over Florida in summer 2004 by comparisons to the Los Alamos Sferic Array, and estimate a mean DE of about 1% for the considered region around 29° N, 82° W. This is in good agreement with our estimated DE for this location in 2004 (0.89%).

A2 DE from concurrent LIS overpasses

In addition to the comparison of WWLLN FRD to the LIS/OTD climatology, we also compared the flashes detected by WWLLN and LIS for individual lightning events. Of course, this approach requires coincident LIS overpass. If we search for LIS overpasses containing the event location within a time window of 2 h before up to 1 h after the event, and demand at least 5 LIS flashes during overpass, we find 42 of such co-

ACPD
10, 18255–18313, 2010

incidences. Two illustrative examples are shown in Figs. 15 and 16, where also TRMM PCTs are shown (see Appendix B).

For each coincidence, we integrate LIS flash counts as well as the respective WWLLN flash counts within the LIS field of view. Figure 14a displays the respective flash counts. In Fig. 14b, corrected flash counts are shown: WWLLN flash counts are scaled by $1/D_{\mathrm{clim}}$, while LIS flash counts are scaled by $1/0.7$, according to the DE of LIS of 70% at 10:00 a.m. Figure 14c displays the "instantaneous" WWLLN DE D_{inst}, defined as ratio of (actual) WWLLN and (corrected) LIS flash counts:

$$D_{\mathrm{inst}} := N_{\mathrm{WWLLN}}/N_{\mathrm{LIS}}^{\mathrm{corr}}, \tag{A1}$$

The ratio of two flash counts for a region of about $640\times640\,\mathrm{km}^2$ (LIS field of view) and a time interval of the order of 1 min (LIS overpass time at the event) is of course rather uncertain, and statistical deviations to the climatological DE are not surprising. Nevertheless, Fig. 14b and c indicate that instantaneous DE are systematically higher (on average by a factor of about 3) than the climatological ones. As WWLLN DE strongly depends on peak current, this finding indicates that the selected events of high lightning activity differ from average lightning with respect to peak current. If this would be the case, the estimated FRD in Fig. 2 are underestimated by a factor of 3. On the other hand, these high-current lightning strokes also likely produce more $\mathrm{LNO_x}$ (Wang et al., 1998). As the dependency of both, DE and $\mathrm{LNO_x}$ production, on peak current is approx. linear for a wide range of peak currents (Rodger et al., 2009; Wang et al., 1998), both effects cancel each other – at least partly – out.

Appendix B

Polarization corrected temperatures from TRMM

There are indications that PE might be related to warm rain vs. mixed-phase precipitation processes (Huntrieser et al., 2009). Thus, in order to investigate the presence

ACPD
10, 18255–18313, 2010

of hail for the detected lightning events, we also analyzed polarization-corrected temperatures (PCT) from brightness temperature measurements of TMI on TRMM for the coincident overpasses as defined in Appendix A. PCT are calculated as defined in Spencer et al. (1989) (Eq. 3 therein). Low PCT are indicators for intense thunderstorms and the presence of hail (Toracinta and Zipser, 2001; Zipser et al., 2006; Cecil, 2009). Figures 15 and 16 show maps of PCT at 37 GHz for two events exemplarily. Flash locations generally coincide with low PCT. Figure 17 shows the correlation of minimum PCT at 37 GHz with (a) minimum PCT at 85 GHz, (b) LIS flash counts, and (c) NO_2 TSCD. PCTs at 37 GHz and 85 GHz are strongly correlated. Minimum PCT at 37/85 GHz reach values down to <180/<70 K, respectively, which are extremely low values (compare Zipser et al., 2006) and are strongly indicating hail (Cecil, 2009). Generally, events with low PCT at 37 GHz also show low PCT at 85 GHz, but for some events PCT at 85 GHz is low (about 100 K), but medium for 37 GHz (about 220 K). LIS flash counts tend to be higher for low PCT, but the scatter is quite high due to the short time interval of LIS overpass. Also the NO_x PE per flash shows a slight tendency to be higher for low PCT, which would correspond to the hypothesis of higher LNO_x PE for flashes from intense thunderstorms. However, the scatter is high ($R=-0.54$), and there are still several cases with low PCT (about 200 K) and low PE.

Appendix C

High NO_2 events

In the discussions of category (A) events (high NO_2 TSCD), we argue that the pattern of enhanced NO_2 for events #115 and #191 can not be explained by fresh LNO_x production alone, but is probably due to aged LNO_x and/or continental outflow of anthropogenic pollution. To support this hypothesis, we additionally analyzed (a) the flashes of the previous 24–48 h, (b) HYSPLIT backtrajectories, and (c) MOPITT CO and SCIAMACHY absorbing aerosol index (AAI) observations.

ACPD
10, 18255–18313, 2010

(a) Figure 18 shows the occurence of WWLLN flashes back to 24 h prior to the SCIAMACHY measurement for events #115 and #191. Note that the clipping shows a larger region compared to Figs. 3 and 4. Again, dots indicate the time of WWLLN flashes relative to the SCIAMACHY measurement, but now back to 24 h. The location of SCIAMACHY pixels and the respective NO_2 TSCD are shown as color-coded rectangles. The pixel of the respective event is marked. High lightning activity can be observed for both events.

(b) Figure 19 shows HYSPLIT backtrajectories, starting at the event, over 48 h for three different altitudes in the middle and upper troposphere. Figure 20 again shows WWLLN lightning activity for the source regions identified by the backtrajectories. For event #191, we actually find indication of deep convection one day back over Houston, Texas (Fig. 20, right), which might have uplifted anthropogenic NO_x to the upper troposphere, from where it might be transported to the event location. For event #115, we can not find indications for such deep convective events over Europe. However, lightning activity around Sicily was very high 2 days before (Fig. 20, left), matching the backtrajectory at 9 km altitude.

(c) Figure 21 shows MOPITT CO VCD and the SCIAMACHY AAI. Both datasets show enhanced values in the vicinity of event #191, but the spatial patterns do not match perfectly. The enhanced CO VCDs might again indicate anthropogenic outflow, but the high AAI clearly indicates biomass burning. In fact, ATSR detected fires in Florida on 11 May 2007.

Thus, though the different datasets do not reveal a simple explanation for the expanded plume of enhanced NO_2 TSCD on 12 May 2007, there is some evidence that this enhancement can not be related to LNO_x alone.

Acknowledgements. Steffen Beirle was funded by the DFG (Deutsche Forschungsgemeinschaft, German research society). We thank ESA and DLR for providing SCIAMACHY spectra. The authors wish to thank the World Wide Lightning Location Network (http://wwlln.net), a collaboration among over 40 universities and institutions, for providing the lightning location data used in this paper. The v1.0 gridded satellite lightning data were produced by the NASA LIS/OTD Science Team (Principal Investigator, Dr. Hugh J. Christian,

ACPD
10, 18255–18313, 2010

NASA/Marshall Space Flight Center) and are available from the Global Hydrology Resource Center (http://ghrc.msfc.nasa.gov). NASA is acknowledged for providing TRMM (http://mirador.gsfc.nasa.gov/) and LIS (http://thunder.nsstc.nasa.gov/data/#LIS_DATA) data. We thank the TEMIS team for providing SCIAMACHY cloud fractions (FRESCO+, http://www.temis.nl). We acknowledge NOAA Air Resources Laboratory for providing the HYSPLIT trajectory model (http://ready.arl.noaa.gov/HYSPLIT.php). MOPITT CO measurements are provided by NASA. SCIAMACHY Aerosol Absorbing Index data was provided by Marloes Penning de Vries. ATSR fire counts were taken from the World Fire Atlas from the Data User Element of the European Space Agency. We thank Craig Rodger and Ken Pickering for helpful discussions.

The service charges for this open access publication
have been covered by the Max Planck Society.

References

Arnone, E., Kero, A., Dinelli, B. M., Enell, C. F., Arnold, N. F., Papandrea, E., Rodger, C. J., Carlotti, M., Ridolfi, M., and Turunen, E.: Seeking sprite-induced signatures in remotely sensed middle atmosphere NO_2, Geophys. Res. Lett., 35, L05807, doi:10.1029/2007GL031791, 2008.

Beirle, S., Platt, U., Wenig, M., and Wagner, T.: NO_x production by lightning estimated with GOME, Adv. Space Res., 34(4), 793–797, 2004.

Beirle, S., Spichtinger, N., Stohl, A., Cummins, K. L., Turner, T., Boccippio, D., Cooper, O. R., Wenig, M., Grzegorski, M., Platt, U., and Wagner, T.: Estimating the NO_x produced by lightning from GOME and NLDN data: a case study in the Gulf of Mexico, Atmos. Chem. Phys., 6, 1075–1089, doi:10.5194/acp-6-1075-2006, 2006.

Beirle, S., Salzmann, M., Lawrence, M. G., and Wagner, T.: Sensitivity of satellite observations for freshly produced lightning NO_x, Atmos. Chem. Phys., 9, 1077–1094, doi:10.5194/acp-9-1077-2009, 2009.

Beirle, S., Kühl, S., Pukīte, J., and Wagner, T.: Retrieval of tropospheric column densities of NO_2 from combined SCIAMACHY nadir/limb measurements, Atmos. Meas. Tech., 3, 283–299, doi:10.5194/amt-3-283-2010, 2010.

ACPD
10, 18255–18313, 2010

Boersma, K. F., Eskes, H. J., and Brinksma, E. J.: Error analysis for tropospheric NO_2 retrieval from space, J. Geophys. Res., 109, D04311, doi:10.1029/2003JD003962, 2004.
Boersma, K. F., Eskes, H. J., Meijer, E. W., and Kelder, H. M.: Estimates of lightning NO_x production from GOME satellite observations, Atmos. Chem. Phys., 5, 2311–2331, doi:10.5194/acp-5-2311-2005, 2005.
Bovensmann, H., Burrows, J. P., Buchwitz, M., Frerick, J., Noël, S., Rozanov, V. V., Chance, K. V., and Goede, A. P. H.: SCIAMACHY: Mission objectives and measurement modes, J. Atmos. Sci., 56(2), 127–150, 1999.
Bucsela, E. J., Pickering, K. E., Huntemann, T. L., Cohen, R. C., Perring, A., Gleason, J. F., Blakeslee, R. J., Albrecht, R. I., Holzworth, R., Cipriani, J. P., Vargas-Navarro, D., Mora-Segura, I., Pacheco-Hernández, A., and Laporte-Molina, S.: Lightning-generated NO_x seen by OMI during NASA's TC4 experiment, J. Geophys. Res., doi:10.1029/2009JD013118, in press, 2010.
Cecil, D. J.: Passive microwave brightness temperatures as proxies for hailstorms, J. Appl. Meteorol. Clim., 48(6), 1281–1286, 2009.
Christian, H. J., Blakeslee, R. J., Boccippio, D. J., et al.: Global frequency and distribution of lightning as observed from space by the Optical Transient Detector, J. Geophys. Res., 108, 4005, doi:10.1029/2002JD002347, 2003.
Cooray, V., Rahman, M., and Rakov, V.: On the NO_x production by laboratory electrical discharges and lightning, J. Atmos. Sol.-Terr. Phy., 71(17–18), 1877–1889, 2009.
Del Genio, A. D., Yao, M.-S., and Jonas, J.: Will moist convection be stronger in a warmer climate?, Geophys. Res. Lett., 34, L16703, doi:10.1029/2007GL030525, 2007.
Dowden, R. L., Brundell, J. B., Rodger, C. J.: VLF lightning location by time of group arrival (TOGA) at multiple sites, J. Atmos. Sol.-Terr. Phy., 64, 817–830, 2002.
Dowden, R. L., Holzworth, R. H., Rodger, C. J., Lichtenberger, J., Thomson, N. R., Jacobson, A. R., Lay, E., Blundell, J. B., Lyons, T. J., O'Keefe, S., Kawasaki, Z., Price, C., Prior, V., Ortega, P., Weinman, J., Mikhailov, Y., Veliz, O., Qie, X., Burns, G., Collier, A., Diaz, R., Adamo, C., Williams, E. R., Kumar, S., Raga, G. B., Rosado, J. M., Avila, E. E., Cliverd, M. A., Ulich, T., Gorham, P., Shanahan, T., Osipowicz, T., Cook, G., and Zhao, Y.: World-wide lightning location using VLF propagation in the Earth-Ionosphere waveguide, IEEE Antenn. Propag. M., 50(5), 40–60, 2008.
Dye, J. E., Ridley, B. A., Skamarock, W., Barth, M., Venticinque, M., Defer, E., Blanchet, P., Thery, C., Laroche, P., Baumann, K., Hubler, G., Parrish, D. D., Ryerson, T., Trainer, M.,

ACPD
10, 18255–18313, 2010

Frost, G., Holloway, J. S., Matejka, T., Bartels, D., Fehsenfeld, F. C., Tuck, A., Rutledge, S. A., Lang, T., Stith, J., and Zerr, R.: An overview of the stratospheric-tropospheric experiment: radiation, aerosols and ozone (STERAO)-deep convection experiment with result from the July 10, 1996 storm, J. Geophys. Res., 105, 10023–10045, 2000.

Hild, L., Richter, A., Rozanov, V., and Burrows, J. P.: Air mass calculations for GOME measurements of lightning-produced NO_2, Adv. Space Res., 29(11), 1685–1690, 2002.

Hudman, R. C., Jacob, D. J., Turquety, S., et al.: Surface and lightning sources of nitrogen oxides over the United States: Magnitudes, chemical evolution, and outflow, J. Geophys. Res., 112, D12S05, doi:10.1029/2006JD007912, 2007.

Huntrieser, H., Schumann, U., Schlager, H., Höller, H., Giez, A., Betz, H.-D., Brunner, D., Forster, C., Pinto Jr., O., and Calheiros, R.: Lightning activity in Brazilian thunderstorms during TROCCINOX: implications for NO_x production, Atmos. Chem. Phys., 8, 921–953, doi:10.5194/acp-8-921-2008, 2008.

Huntrieser, H., Schlager, H., Lichtenstern, M., Roiger, A., Stock, P., Minikin, A., Höller, H., Schmidt, K., Betz, H.-D., Allen, G., Viciani, S., Ulanovsky, A., Ravegnani, F., and Brunner, D.: NO_x production by lightning in Hector: first airborne measurements during SCOUT-O3/ACTIVE, Atmos. Chem. Phys., 9, 8377–8412, doi:10.5194/acp-9-8377-2009, 2009.

Jacobson, A., Holzworth, R., Harlin, J., Dowden, R., and Lay, E.: Performance assessment of the World Wide Lightning Location Network (WWLLN), using the Los Alamos Sferic Array (LASA) as ground truth, J. Atmos. Ocean. Technol., 23(8), 1082–1092, 2006.

Labrador, L. J., von Kuhlmann, R., and Lawrence, M. G.: The effects of lightning-produced NO_x and its vertical distribution on atmospheric chemistry: sensitivity simulations with MATCH-MPIC, Atmos. Chem. Phys., 5, 1815–1834, doi:10.5194/acp-5-1815-2005, 2005.

Langford, A. O., Portmann, R. W., Daniel, J. S., Miller, H. L., and Solomon, S.: Spectroscopic measurements of NO_2 in a Colorado thunderstorm: Determination of the mean production by cloud-to-ground lightning flashes, J. Geophys. Res., 109, D11304, doi:10.1029/2003JD004158, 2004.

Lay, E. H., Holzworth, R. H., Rodger, C. J., Thomas, J. N., Pinto Jr., O., Dowden, R. L.: WWLL global lightning detection system: Regional validation study in Brazil, Geophys. Res. Lett., 31(3), doi:10.1029/2003GL018882, 2004.

Lay, E. H., Jacobson, A. R., Holzworth, R. H., Rodger, C. J., and Dowden, R. L.: Local time variation in land/ocean lightning flash density as measured by the World Wide Lightning Location Network, J. Geophys. Res., 112, D13111, doi:10.1029/2006JD007944, 2007.

ACPD
10, 18255–18313, 2010

LIS/OTD documentation: LIS/OTD Gridded Products V 2.2: 1995–2005, Documentation and Examples, 1 September 2006, http://ghrc.nsstc.nasa.gov/uso/ds_docs/lis_climatology/lis_otd_gridded_products_documentation_v2.2.pdf, last access: March 2010, 2007.

Martin, R. V., Chance, K., Jacob, D. J., Kurosu, T. P., Spurr, R. J. D., Bucsela, E., Gleason, J. F., Palmer, P. I., Bey, I., Fiore, A. M., Li, Q., Yantosca, R. M., and Koelemeijer, R. B. A.: An improved retrieval of tropospheric nitrogen dioxide from GOME, J. Geophys. Res., 107(D20), 4437, doi:10.1029/2001JD001027, 2002.

Martin, R. V., Sauvage, B., Folkins, I., Sioris, C. E., Boone, C., Bernath, P., Ziemke, J.: Space-based constraints on the production of nitric oxide by lightning, J. Geophys. Res., 112, D09309, doi:10.1029/2006JD007831, 2007.

Martin, R. V.: Satellite remote sensing of surface air quality, Atmos. Environ., 42, 7823–7843, 2008.

Ott, L. E., Pickering, K. E., Stenchikov, G. L., Allen, D. J., DeCaria, A. J., Ridley, B., Lin, R.-F., Lang, S., and Tao, W.-K.: Production of lightning NO_x and its vertical distribution calculated from three-dimensional cloud-scale chemical transport model simulations, J. Geophys. Res., 115, D04301, doi:10.1029/2009JD011880, 2010.

Penning de Vries, M. J. M., Beirle, S., and Wagner, T.: UV Aerosol Indices from SCIAMACHY: introducing the SCattering Index (SCI), Atmos. Chem. Phys., 9, 9555–9567, doi:10.5194/acp-9-9555-2009, 2009.

Price, C. and Rind, D.: What determines the cloud-to-ground lightning fraction in thunderstorms?, Geophys. Res. Lett., 20, 463–466, 1993.

Rahman, M., Cooray, V., Rakov, V. A., Uman, M. A., Liyanage, P., DeCarlo, B. A., Jerauld, J., and Olsen, R. C.: Measurements of NO_x produced by rocket-triggered lightning, Geophys. Res. Lett., 34, L03816, doi:10.1029/2006GL027956, 2007.

Rodger, C. J., Brundell, J. B., Dowden, R. L., and Thomson, N. R.: Location accuracy of long distance VLF lightning locationnetwork, Ann. Geophys., 22, 747–758, doi:10.5194/angeo-22-747-2004, 2004.

Rodger, C. J., Werner, S., Brundell, J. B., Lay, E. H., Thomson, N. R., Holzworth, R. H., and Dowden, R. L.: Detection efficiency of the VLF World-Wide Lightning Location Network (WWLLN): initial case study, Ann. Geophys., 24, 3197–3214, doi:10.5194/angeo-24-3197-2006, 2006.

Rodger, C. J., Brundell, J. B., Holzworth, R. H., and Lay, E. H.: Growing Detection Efficiency of the World Wide Lightning Location Network, Am. Inst. Phys. Conf. Proc., Coupling of

ACPD
10, 18255–18313, 2010

thunderstorms and lightning discharges to near-Earth space: Proceedings of the Workshop, Corte (France), 23–27 June 2008, 1118, 15–20, doi:10.1063/1.3137706, 2009.
Scargle, J. D.: Publication bias: the file-drawer problem in scientific inference, J. Sci. Explor., 14(2), 94–106, 2000.
Schumann, U. and Huntrieser, H.: The global lightning-induced nitrogen oxides source, Atmos. Chem. Phys., 7, 3823–3907, doi:10.5194/acp-7-3823-2007, 2007.
Spencer, R. W., Goodman, H. M., and Hood, R. E.: Precipitation retrieval over land and ocean with the SSM/I: Identification and characteristics of the scattering signal, J. Atmos. Ocean. Tech., 6, 254–273, 1989.
Wagner, T., Beirle, S., Deutschmann, T., Eigemeier, E., Frankenberg, C., Grzegorski, M., Liu, C., Marbach, T., Platt, U., and Penning de Vries, M.: Monitoring of atmospheric trace gases, clouds, aerosols and surface properties from UV/vis/NIR satellite instruments, J. Opt. A, Pure Appl. Opt., 10, 104019, doi:10.1088/1464-4258/10/10/104019, 2008.
Wang, Y., DeSilva, A. W., Goldenbaum, G. C., and Dickerson, R. R.: Nitric oxide production by simulated lightning: Dependence on current, energy, and pressure, J. Geophys. Res., 103, 19149–19159, 1998.
Wang, P., Stammes, P., van der A, R., Pinardi, G., and van Roozendael, M.: FRESCO+: an improved O_2 A-band cloud retrieval algorithm for tropospheric trace gas retrievals, Atmos. Chem. Phys., 8, 6565–6576, doi:10.5194/acp-8-6565-2008, 2008.
Zipser, E. J., Cecil, D. J., Liu, C., Nesbitt, S. W., and Yorty, D. P.: Where are the most intense thunderstorms on Earth?, Bull. Amer. Meteorol. Soc., 87, 1057–1071, 2006.

ACPD
10, 18255–18313, 2010

Table 1. List of acronyms and symbols used in this study.

Symbol	Acronym	Explanation
	LIS	Lightning imaging sensor
	OTD	Optical transient detector
	SCIAMACHY	Scanning Imaging Absorption spectroMeter for Atmospheric CHartographY
	TMI	TRMM microwave imager
	TRMM	Tropical rainfall measuring mission
	WWLLN	World Wide Lightning Location Network
	CG	Cloud-to-ground flash
	IC	Intra-cloud
	PCT	Polarization-corrected temperature
S	TSCD	Tropospheric slant column density
V	TVCD	Tropospheric vertical column density
E		Sensitivity (see Eq. 1)
F	FRD	Flash rate density
D	DE	Detection efficiency
P	PE	Production efficiency (LNO_x per flash)

ACPD
10, 18255–18313, 2010

Table 2. Selected events of high lightning activity (compare Figs. 3–8 and Sect. 2.4)

Event ID	Date	FRD $[\frac{1}{km^2 h}]$	NO_2 TSCD $[10^{15} \frac{molec}{cm^2}]$	PE $[10^{25} \frac{molec}{flash}]$	WWLLN DE [%]	Latitude [°]	Longitude [°]	Cloud fraction	Cloud height [km]
#115	16 Oct 2006	2.9	4.6	3.5	5.5	35.3	17.5	1.0	10.9
#191	5 Dec 2007	1.0	5.8	12.3	15.7	24.9	−71.9	1.0	10.4
#208	20 Aug 2007	5.8	0.5	0.2	7.2	2.1	108.2	1.0	12.1
#225	22 Nov 2007	2.2	2.4	2.3	10.7	−7.4	125.7	1.0	12.6
#261	13 May 2008	1.7	2.3	2.9	12.7	6.2	106.4	1.0	12.7
#266	15 Jul 2008	1.0	0.3	0.7	11.3	15.4	−71.6	1.0	11.2

ACPD
10, 18255–18313, 2010

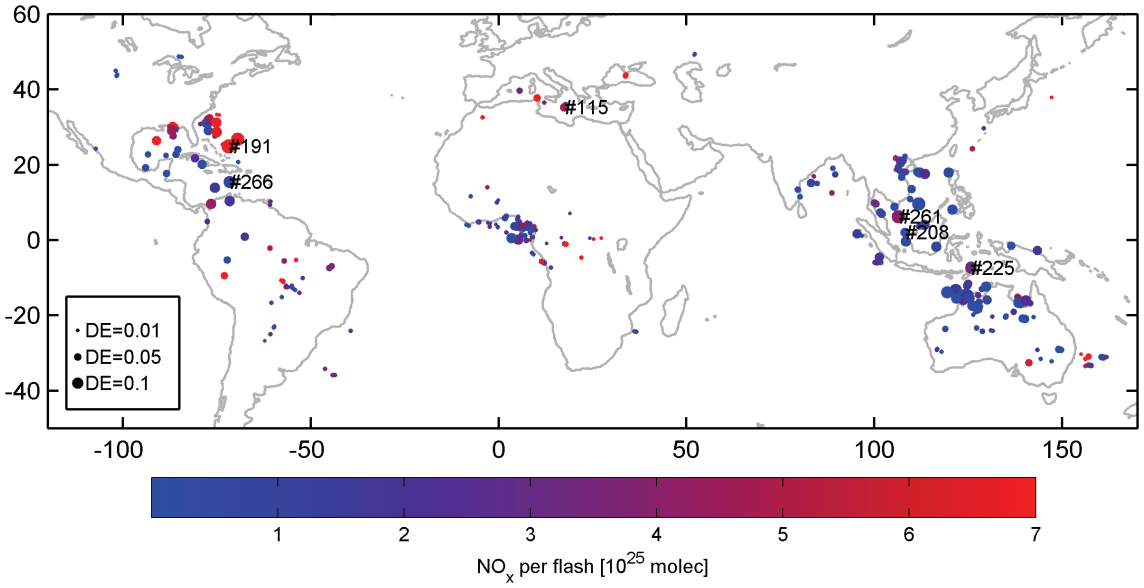

Fig. 1. Global map of events of high lightning activity coinciding with SCIAMACHY overpasses. The colors indicate the production efficiency, i.e. the LNO_x production per flash P_{event}, for the assumptions made (see Sect. 2.4). The size of the circles indicates the estimated WWLLN DE D_{clim}. Some selected events, which are discussed in detail below, are labelled by their event ID.

ACPD
10, 18255–18313, 2010

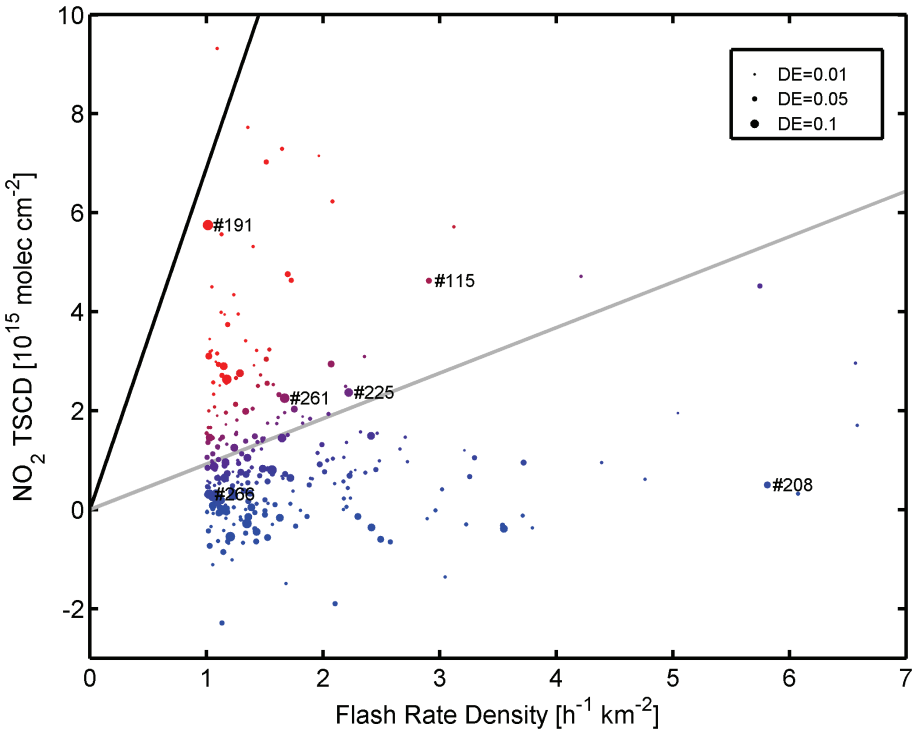

Fig. 2. NO_2 TSCDs for the events of high lightning activity with FRD>1/km^2/h. Colors, coding P_{event}, as in Fig. 1. The black line reflects the expectation (according to Eqs. 1 and 4) of 6.9×10^{15} molec/cm^2 per 1/km^2/h, or $P=15\times10^{15}$ molec/flash. The grey line represents the lower bound according to P of 2×10^{15} molec/flash given in Schumann and Huntrieser (2007).

ACPD
10, 18255–18313, 2010

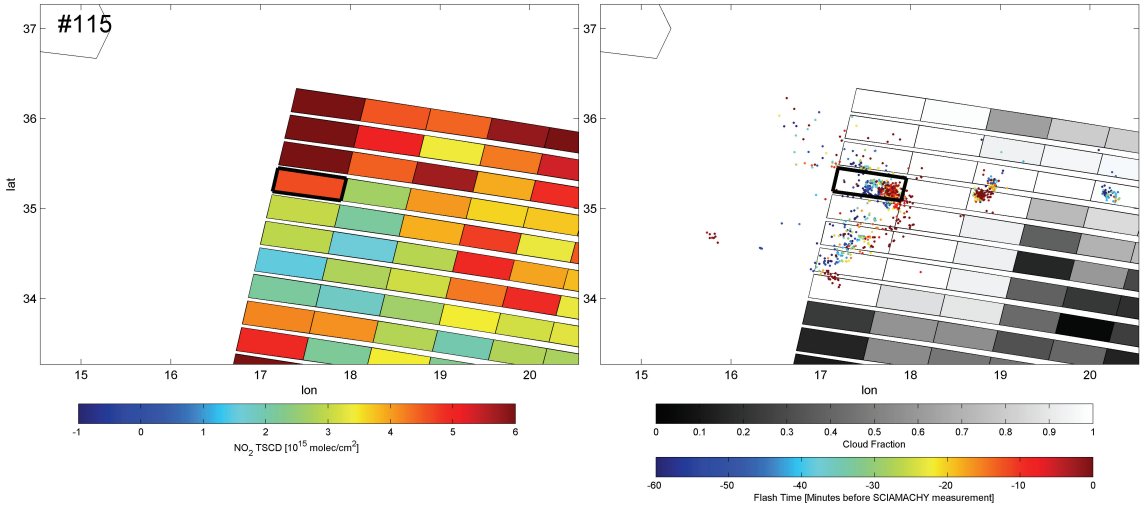

Fig. 3. Event #115 on 16 October 2006. Left: NO_2 TSCD. Right: Cloud fraction (greyscale) and time of individual WWLLN flashes relative to the SCIAMACHY measurement (color).

ACPD
10, 18255–18313, 2010

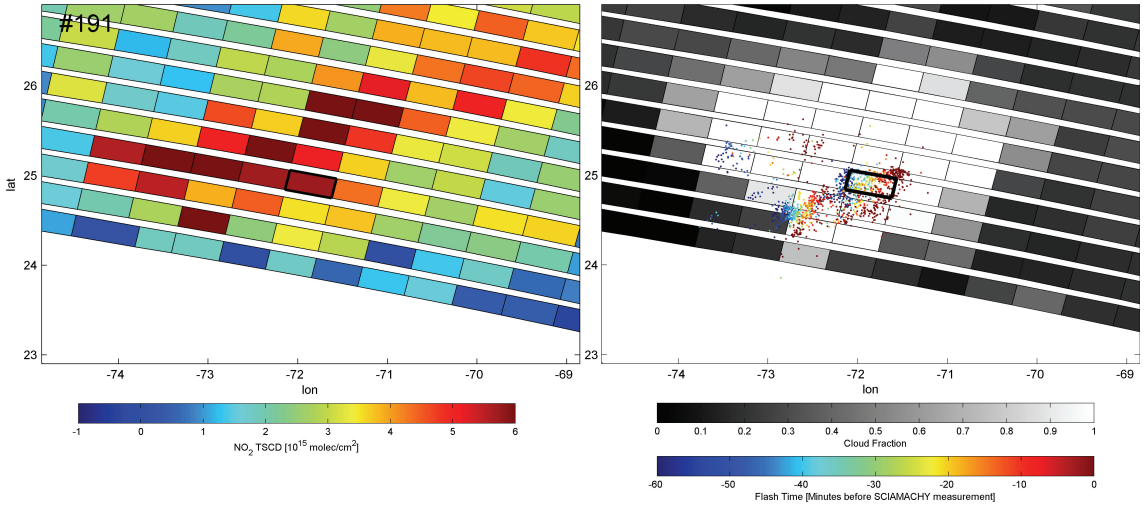

Fig. 4. Event #191 on 12 May 2007. Left: NO_2 TSCD. Right: Cloud fraction (greyscale) and time of individual WWLLN flashes relative to the SCIAMACHY measurement (color).

ACPD
10, 18255–18313, 2010

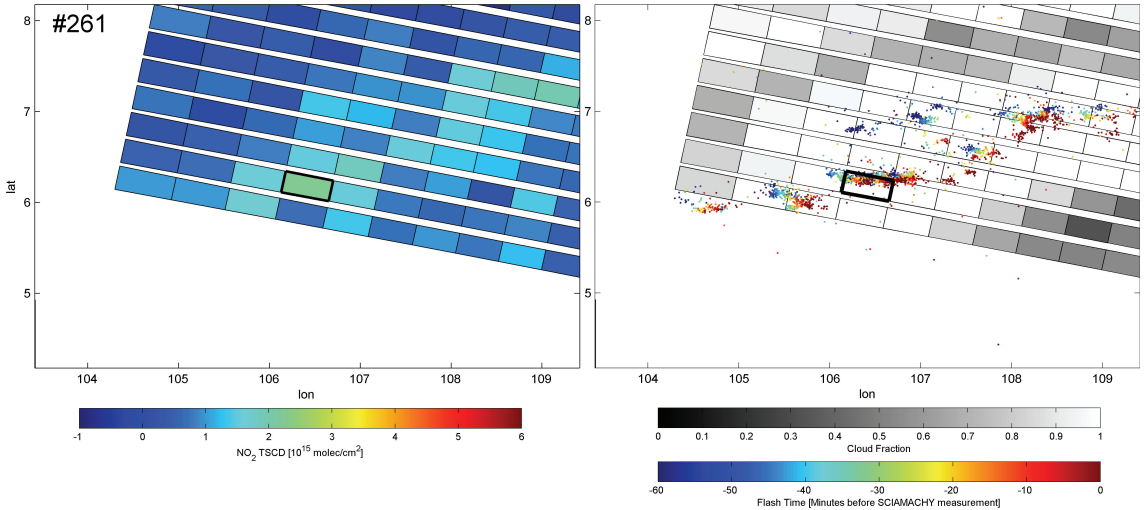

Fig. 5. Event #261 on 13 May 2008. Left: NO_2 TSCD. Right: Cloud fraction (greyscale) and time of individual WWLLN flashes relative to the SCIAMACHY measurement (color).

ACPD
10, 18255–18313, 2010

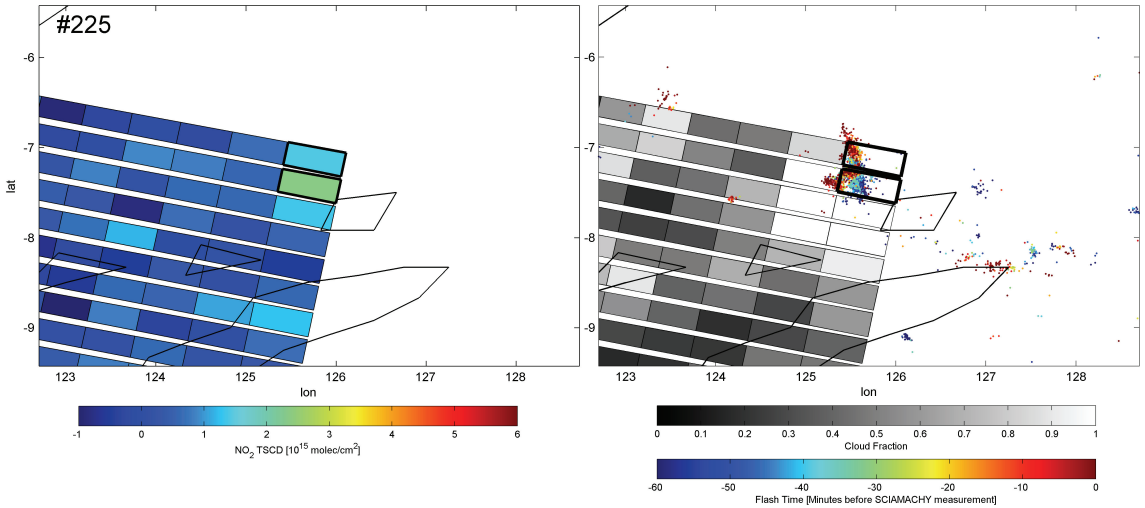

Fig. 6. Event #225 on 22 November 2007. Left: NO_2 TSCD. Right: Cloud fraction (greyscale) and time of individual WWLLN flashes relative to the SCIAMACHY measurement (color).

ACPD
10, 18255–18313, 2010

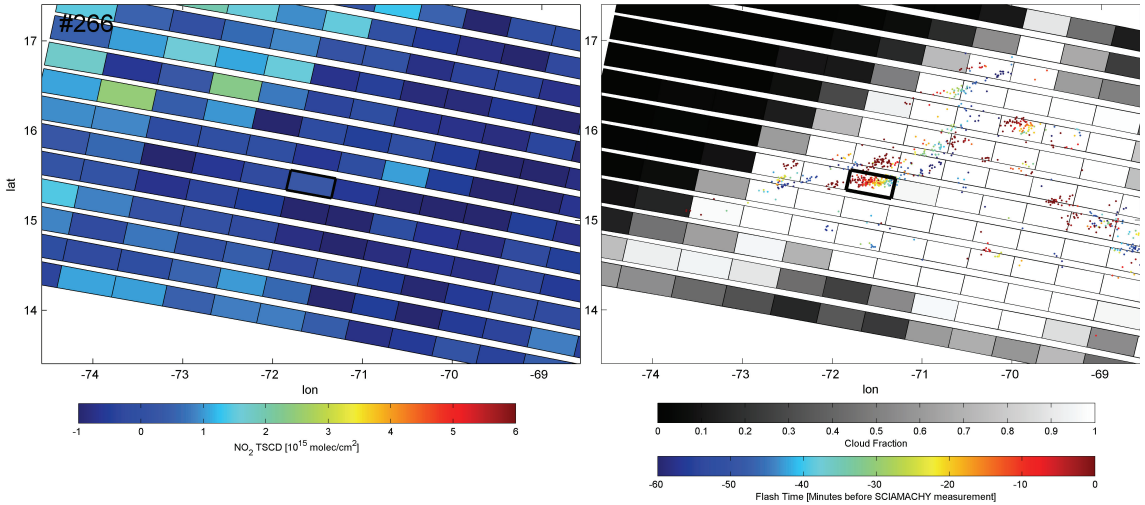

Fig. 7. Event #266 on 15 July 2008. Left: NO_2 TSCD. Right: Cloud fraction (greyscale) and time of individual WWLLN flashes relative to the SCIAMACHY measurement (color).

ACPD
10, 18255–18313, 2010

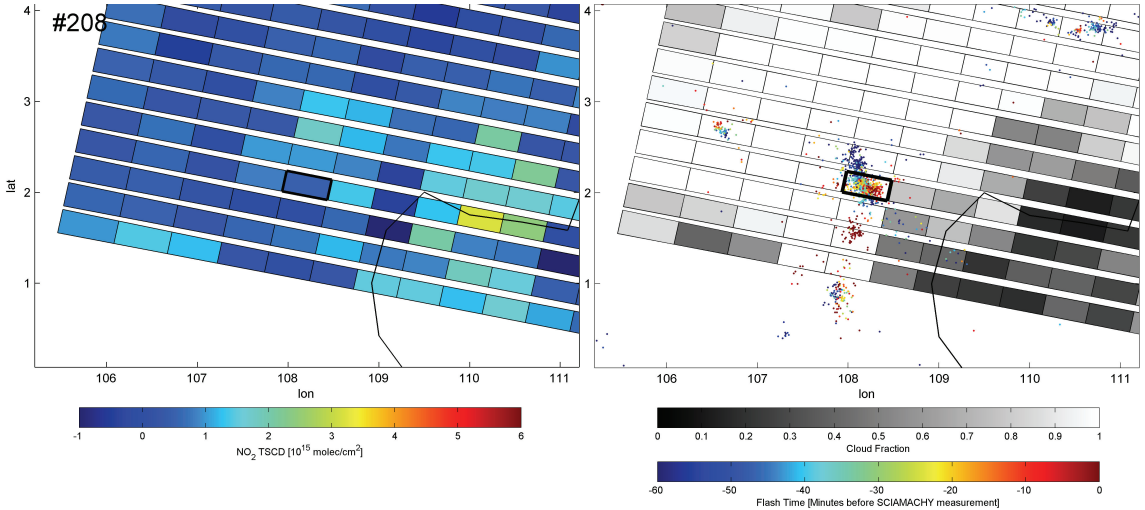

Fig. 8. Event #208 on 20 August 2007. Left: NO_2 TSCD. Right: Cloud fraction (greyscale) and time of individual WWLLN flashes relative to the SCIAMACHY measurement (color).

ACPD
10, 18255–18313, 2010

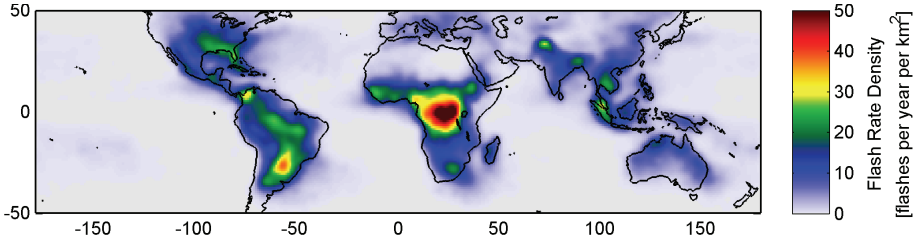

Fig. 9. Global map of the LIS climatology flash rate density.

ACPD
10, 18255–18313, 2010

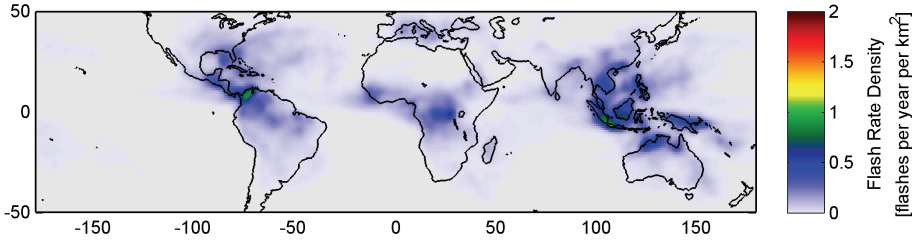

Fig. 10. Global map of the WWLLN flash rate density in 2005 (uncorrected).

ACPD
10, 18255–18313, 2010

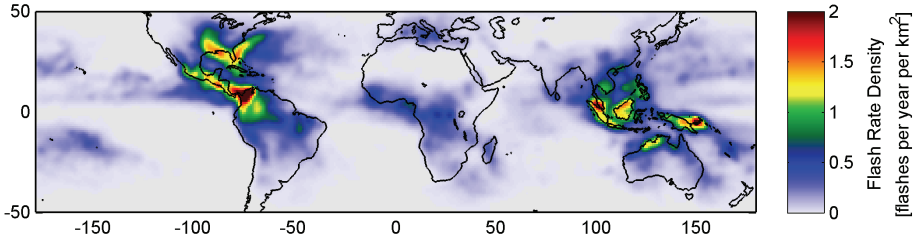

Fig. 11. Global map of the WWLLN flash rate density in 2008 (uncorrected).

ACPD
10, 18255–18313, 2010

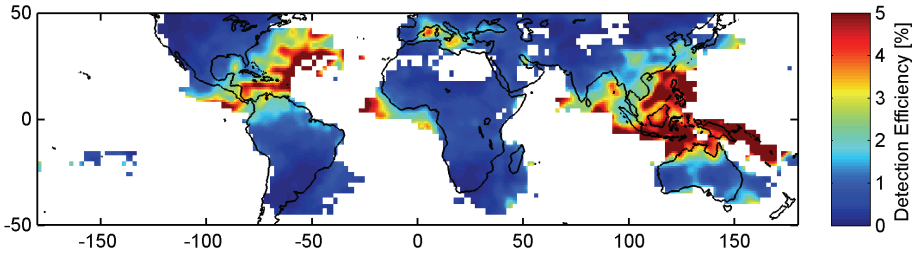

Fig. 12. Global map of the WWLLN detection efficiency D_{clim} for 2005.

ACPD
10, 18255–18313, 2010

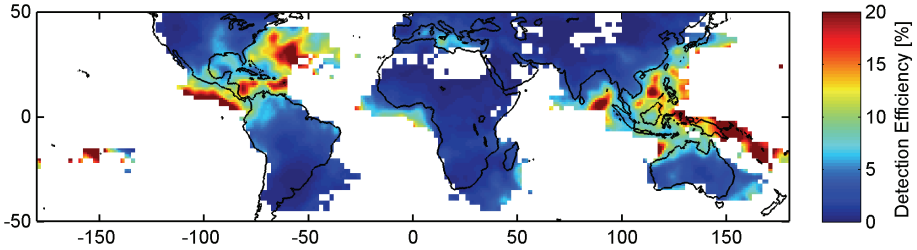

Fig. 13. Global map of the WWLLN detection efficiency D_{clim} for 2008. Note the changed colorscale compared to Fig. 12.

ACPD
10, 18255–18313, 2010

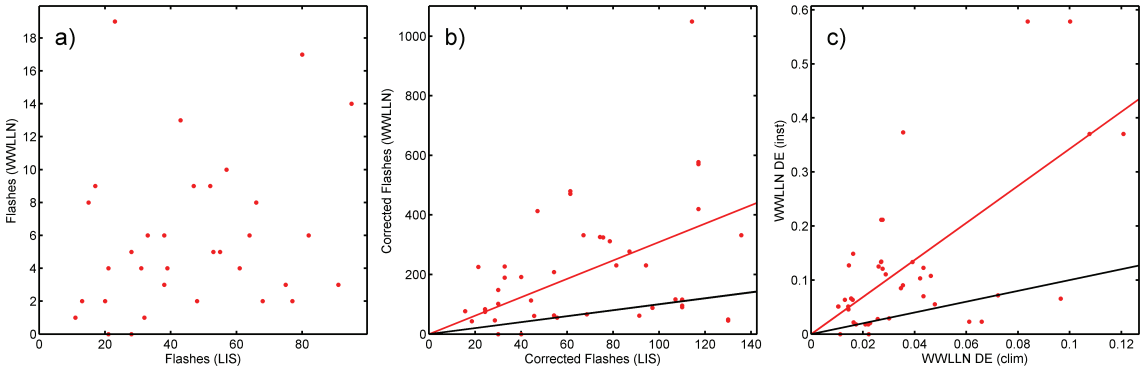

Fig. 14. Comparison of flash counts from LIS and WWLLN for LIS overpasses coinciding with SCIAMACHY for events of high lightning activity. **(a)** Scatterplot of original flash counts from LIS and WWLLN. **(b)** Correlation (R=0.35) of corrected flash counts from LIS (scaled by 1/0.7) and WWLLN (scaled by $1/D_{\mathrm{clim}}$). The black line corresponds to 1:1. The slope of the fitted line through origin (red) is 3.1. **(c)** Correlation (R=0.63) of D_{clim} (Eq. 2) and D_{inst} (Eq. A1). The black line corresponds to 1:1. The slope of the fitted line through origin (red) is 3.4.

ACPD
10, 18255–18313, 2010

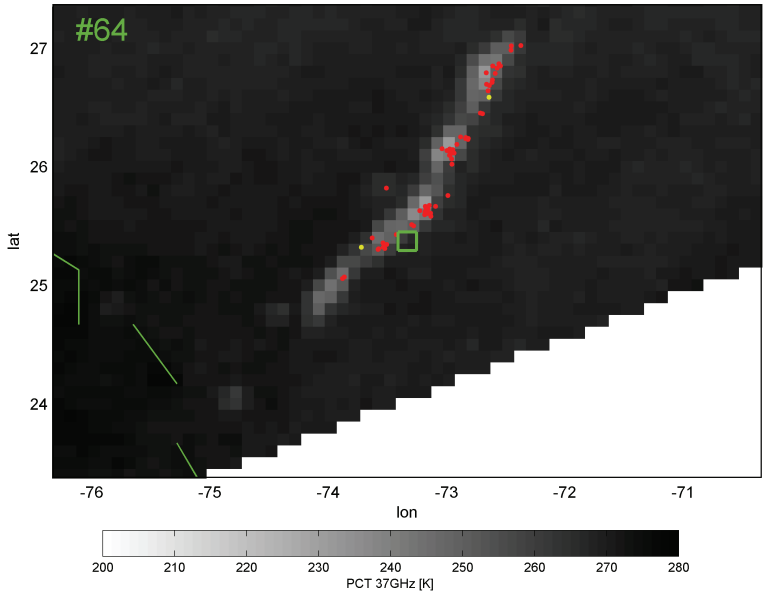

Fig. 15. TRMM overpass 99 min before event #64 (11 September 2005, east of Florida). Greyscale background shows the PCT at 37 GHz, with a minimum of 228 K. Red dots are flashes detected by LIS (68 in total), while yellow dots are WWLLN flashes (2 in total) detected within the LIS overpass time. The green square marks the center coordinates of the SCIAMACHY pixel for event #64. The respective climatological DE is 2.3%, while the instantaneous DE is 2/(68/0.7)=2.1%.

ACPD
10, 18255–18313, 2010

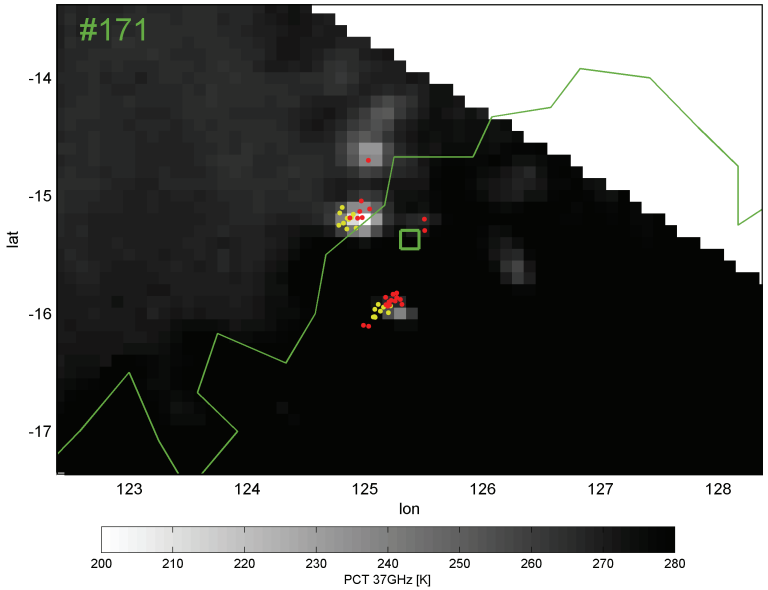

Fig. 16. TRMM overpass 43 min after event #171 (4 March 2007, Northern Australia). Greyscale background shows the PCT at 37 GHz, with a minimum of 199 K. Red dots are flashes detected by LIS (23 in total), while yellow dots are WWLLN flashes (19 in total) detected within the LIS overpass time. The green square marks the center coordinates of the SCIAMACHY pixel for event #171. The respective climatological DE is 8.4%, while the instantaneous DE is 19/(23/0.7)=57.8%.

ACPD
10, 18255–18313, 2010

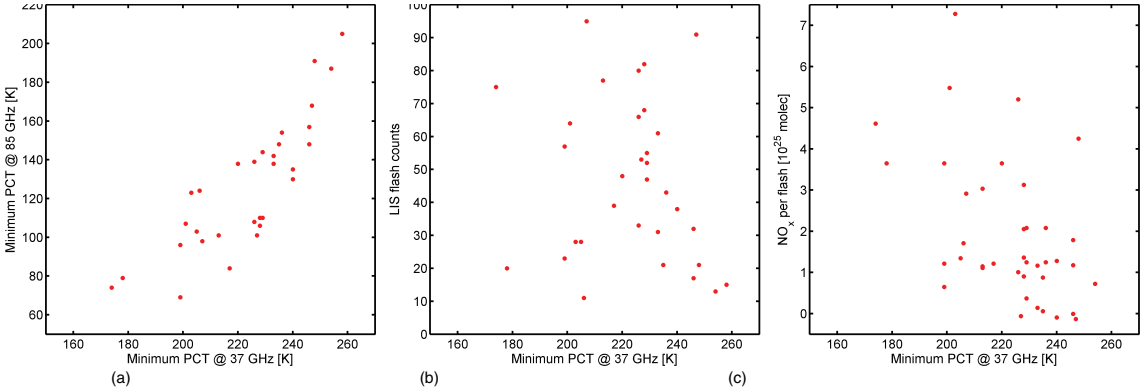

Fig. 17. Correlation of minimum PCT at 37 GHz with **(a)** minimum PCT at 85 GHz (R=0.84), **(b)** number of LIS flash counts (R=−0.13), and **(c)** the production efficiency P_{event} (R=−0.54), for the coincident TRMM overpasses.

ACPD
10, 18255–18313, 2010

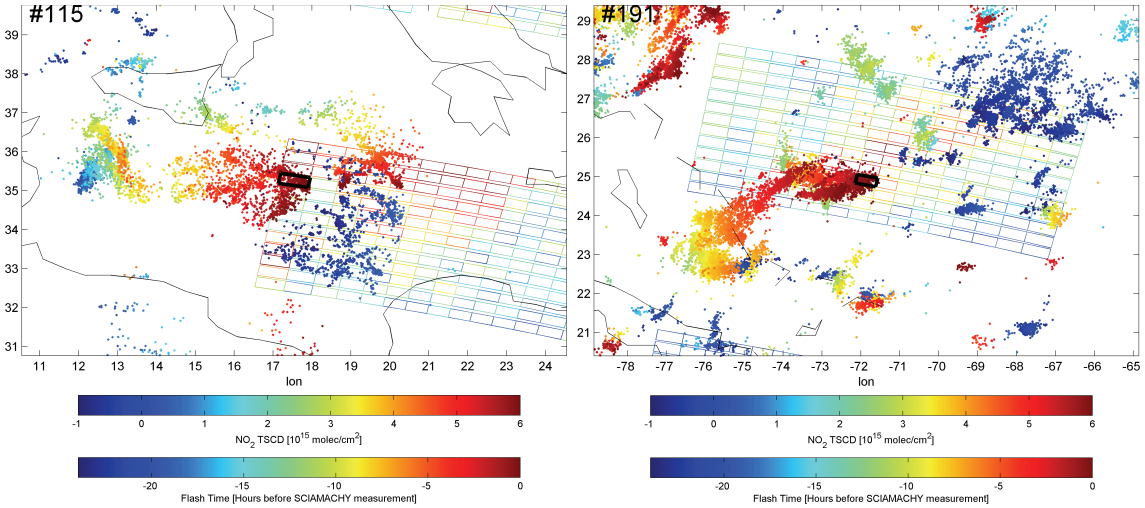

Fig. 18. Occurence of WWLLN flashes back to 24 h prior to the SCIAMACHY measurement for events #115 (left) and #191 (right). Note that the clipping shows a larger region compared to Figs. 3 and 4. Dots indicate the time of WWLLN flashes relative to the SCIAMACHY measurement back to 24 h. The location of SCIAMACHY pixels and the respective NO_2 TSCD are shown as color-coded rectangles. The pixel of the respective event of high lightning activity is marked.

ACPD
10, 18255–18313, 2010

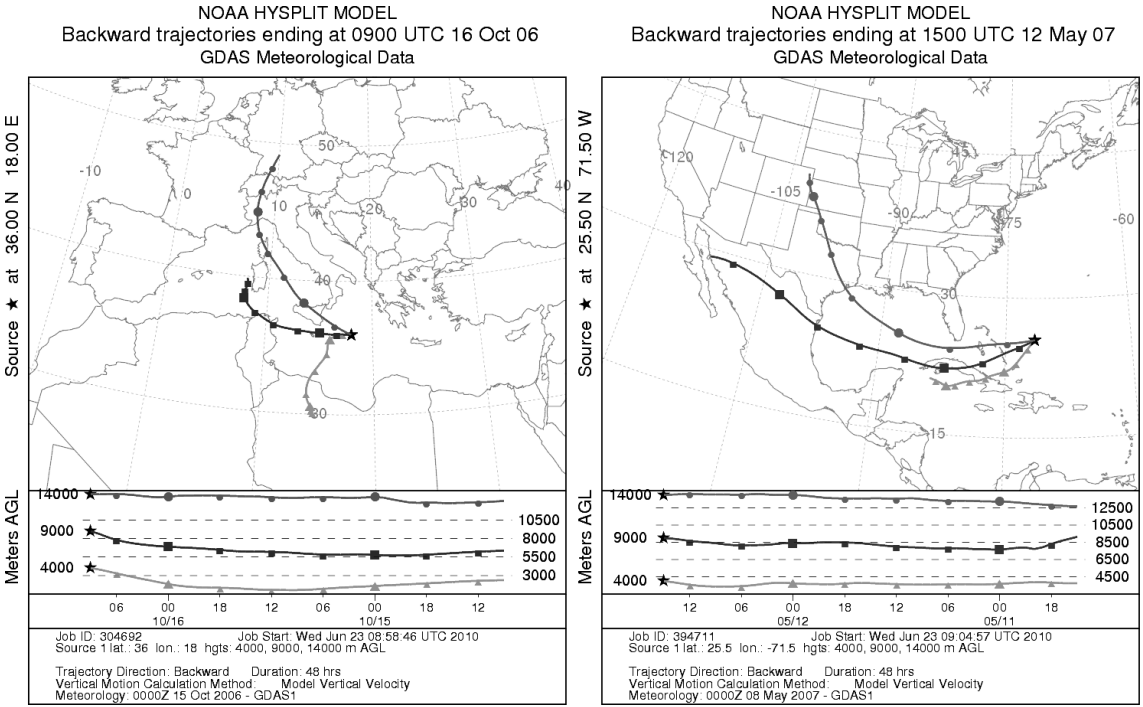

Fig. 19. HYSPLIT backtrajectories from the event location over 48 h for 3 different altitudes for events #115 (left) and #191 (right). Air-masses of continental (polluted) origin can only be identified for transport in the upper troposphere.

ACPD
10, 18255–18313, 2010

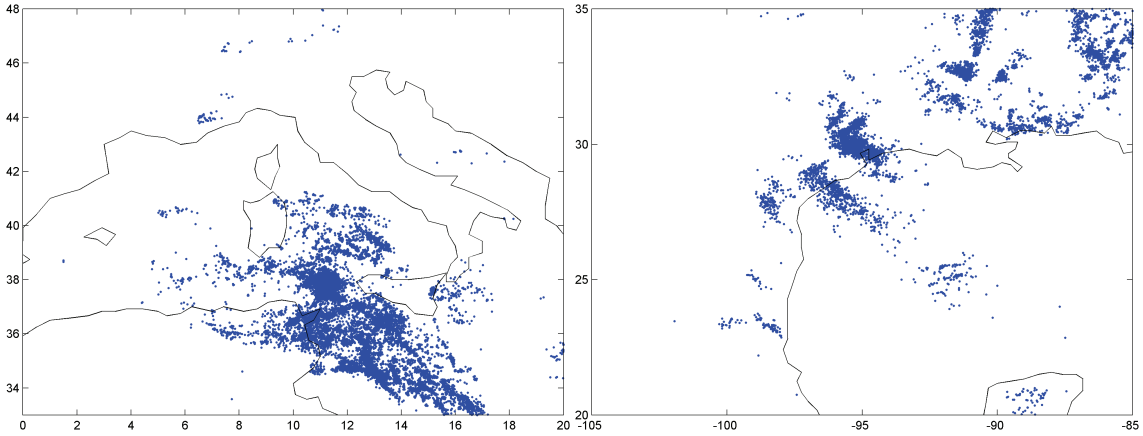

Fig. 20. WWLLN flash counts over the area covered by the HYSPLIT backtrajectories for 14 October 2006 (left) and 11 May 2007 (right), i.e. 1–2 d before the respective events. In case of event #191, there was high lightning activity, indicating deep convection, around Houston, which matches the track of the backward trajectory at 14 km altitude. For event #115, no comparable convection over polluted European regions could be found. Instead, very high lightning activity is observed south and west from Sicily, matching the backward trajectory at 9 km.

ACPD
10, 18255–18313, 2010

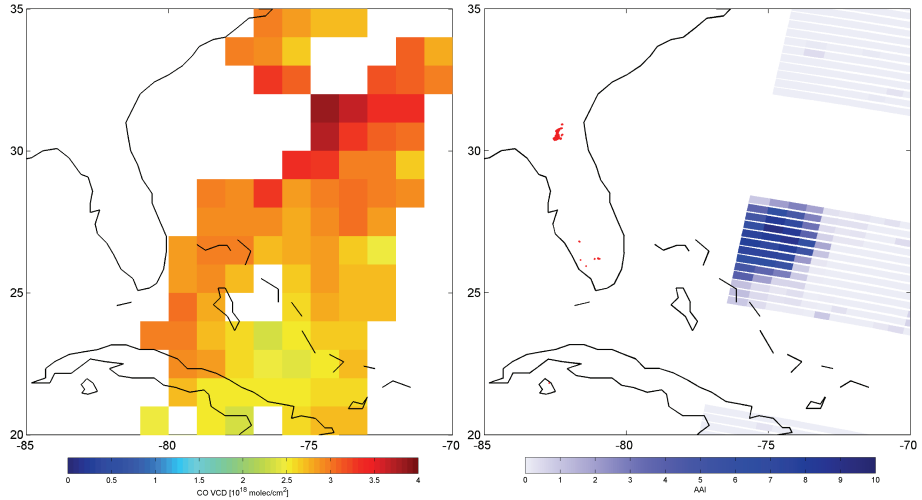

Fig. 21. Left: MOPITT CO VCD on 12 May 2007. Right: SCIAMACHY absorbing aerosol index (AAI) (Penning de Vries et al., 2009) on 12 May 2007. The red dots indicate fires detected by ATSR on 11 May 2007.

ACPD
10, 18255–18313, 2010